Southern Hemisphere Additional Ozonesondes (SHADOZ) 1998–2000 tropical ozone climatology
2. Tropospheric variability and the zonal wave-one

Anne M. Thompson,[1] Jacquelyn C. Witte,[1,2] Samuel J. Oltmans,[3] Francis J. Schmidlin,[4] Jennifer A. Logan,[5] Masatomo Fujiwara,[6] Volker W. J. H. Kirchhoff,[7] Françoise Posny,[8] Gert J. R. Coetzee,[9] Bruno Hoegger,[10] Shuji Kawakami,[11] Toshihiro Ogawa,[11] J. P. F. Fortuin,[12] and H. M. Kelder[12,13]

[1] The first view of stratospheric and tropospheric ozone variability in the Southern Hemisphere tropics is provided by a 3-year record of ozone soundings from the Southern Hemisphere Additional Ozonesondes (SHADOZ) network (http://croc.gsfc.nasa.gov/shadoz). Observations covering 1998–2000 were made over Ascension Island, Nairobi (Kenya), Irene (South Africa), Réunion Island, Watukosek (Java), Fiji, Tahiti, American Samoa, San Cristóbal (Galapagos), and Natal (Brazil). Total, stratospheric, and tropospheric column ozone amounts usually peak between August and November. Other features are a persistent zonal wave-one pattern in total column ozone and signatures of the quasi-biennial oscillation (QBO) in stratospheric ozone. The wave-one is due to a greater concentration of free tropospheric ozone over the tropical Atlantic than the Pacific and appears to be associated with tropical general circulation and seasonal pollution from biomass burning. Tropospheric ozone over the Indian and Pacific Oceans displays influences of the waning 1997–1998 El Niño, seasonal convection, and pollution transport from Africa. The most distinctive feature of SHADOZ tropospheric ozone is variability in the data, e.g., a factor of 3 in column amount at 8 of 10 stations. Seasonal and monthly means may not be robust quantities because statistics are frequently not Gaussian even at sites that are always in tropical air. Models and satellite retrievals should be evaluated on their capability for reproducing tropospheric variability and fine structure. A 1999–2000 ozone record from Paramaribo, Surinam (6°N, 55°W) (also in SHADOZ) shows a marked contrast to southern tropical ozone because Surinam is often north of the Intertropical Convergence Zone (ITCZ). A more representative tropospheric ozone climatology for models and satellite retrievals requires additional Northern Hemisphere tropical data. *INDEX TERMS:* 0365 Atmospheric Composition and Structure: Troposphere—composition and chemistry; 1640 Global Change: Remote sensing; 3309 Meteorology and Atmospheric Dynamics: Climatology (1620); 9305 Information Related to Geographic Region: Africa; 9325 Information Related to Geographic Region: Atlantic Ocean; *KEYWORDS:* Free-words-ozone, tropospheric ozone, ozonesondes, satellite ozone, tropical climatology, wave-one, biomass burning, El Niño, satellite retrievals

Citation: Thompson, A. M., et al., Southern Hemisphere Additional Ozonesondes (SHADOZ) 1998–2000 tropical ozone climatology, 2, Tropospheric variability and the zonal wave-one, *J. Geophys. Res.*, *108*(D2), 8241, doi:10.1029/2002JD002241, 2003.

1. Introduction

[2] Tropical ozone is an active player in atmospheric chemistry and dynamics. Ozone profile data are remarkably rich in information about atmospheric transport. In the upper troposphere, ozone is a greenhouse gas that plays a key role in radiative forcing and potential climate change [*Wang et al.*, 1980, 1993; *Hansen et al.*, 2002]. Thus, ozone

---

[1]NASA Goddard Space Flight Center, Greenbelt, Maryland, USA.
[2]Also at Science Systems and Applications, Inc., Lanham, Maryland, USA.
[3]NOAA Climate Monitoring and Diagnostics Laboratory, Boulder, Colorado, USA.
[4]NASA Wallops Flight Facility, Wallops Island, Virginia, USA.
[5]Department of Earth and Planetary Sciences, Harvard University, Cambridge, Massachusetts, USA.

[6]Radio Science Center for Space and Atmosphere, Kyoto University, Kyoto, Japan.
[7]INPE Laboratorio Ozonio, São José dos Campos, Brazil.
[8]Université de la Réunion, St.-Denis, Réunion, France.
[9]South African Weather Service, Pretoria, South Africa.
[10]Swiss Aerological Observatory, Payerne, Switzerland.
[11]NASDA Earth Observations Research Center, Tokyo, Japan.
[12]Royal Netherlands Meteorological Institute, De Bilt, Netherlands.
[13]Einhoven Technical University, Einhoven, Netherlands.

Table 1. Major Tropical Campaigns With Ozone Measurements

Region	Acronym [Publication]
South America–Atlantic–Africa	TROPOZ [*J. Geophys. Res., 103*(D15), 1998]
	ABLE-2A, ABLE-2B (Amazon Boundary Layer Experiments) [*J. Geophys. Res., 93*(D2), 1998; *Kirchhoff et al.*, 1990]
	DECAFE (Dynamique et Chimie en Afrique Experiment) [*J. Geophys. Res., 97*(D6), 1992]
	SAFARI-92/TRACE-A (Southern African Fire Atmospheric Research Initiative/Transport and Atmospheric Chemistry near the Equator-Atlantic) [*J. Geophys. Res., 101*(D19), 1996]
	SCAR-B (Smoke, Clouds and Radiation-Brazil) [*J. Geophys. Res., 103*(D24), 1998]
	LBA-CLAIRE [*J. Atmos. Chem., 39*(1), 2001]
	SAFARI-2000 [*Swap et al.*, 2002]
	Polarstern cruises (1987, 1988) [*Smit et al.*, 1989; *Weller et al.*, 1996], Aerosols99 cruise [*Thompson et al.*, 2000]
Pacific	ASHOE/MAESA (Airborne Southern Hemisphere Ozone Experiment/Mission for Atmospheric Effects of Stratospheric Aviation) [*J. Geophys. Res., 102*(D3), 1997]
	TOTE/VOTE [*Geophys. Res. Lett., 25*(5), 1998]
	STRAT [*J. Geophys. Res., 104*(D21), 1999]
	PEM-Tropics A [*J. Geophys. Res., 104*(D5), 1999]
	PEM-Tropics B [*J. Geophys. Res., 106*(D23), 2001]
	Cruises: SAGA-3 [*J. Geophys. Res., 98*(D9), 1993];
	CEPEX [*Q. J. R. Meteorol. Soc., 123*(543) Part A, 1997]
Indian Ocean, Maritime Continent	STEP (Stratospheric–Tropospheric Experiment 1987) [*J. Geophys. Res., 98*(D5), 1993]
	INDOEX-1999 [*Lelieveld et al.*, 2001, *J. Geophys. Res., 106*(D22), 2001]
	BIBLE-A/B (1998–1999) [*Kondo et al.*, 2002]

profile data are needed to determine whether or not ozone is increasing or decreasing [*WMO/SPARC*, 1998]. Tracer studies, i.e., measurements of ozone with aerosols, CO, H_2O, or with trajectories, allow determination of the "age" and origins of air parcels.

[3]   Ozone profile observations are typically made in three ways. (1) Field campaigns with in situ measurements from aircraft, ground-based, and similar platforms capture ozone in certain regions and under various conditions. Intensive campaigns are required to quantify processes but give a limited regional view and only a snapshot in time. Examples of campaigns that have studied tropical ozone under various conditions are listed in Table 1.

[4]   (2) Satellite observations represent one extreme from campaign sampling by offering global coverage. There are a number of stratospheric ozone profiling satellite instruments. Tropospheric ozone in the tropics is now derived in near real time (http://www.atmos.umd.edu/~tropo), allowing us to follow, for example, transboundary pollution from biomass fires [*Thompson et al.*, 2001]. The drawback to satellite measurements is that, at present, only column amounts can be retrieved in the troposphere. Gradients and layers that give evidence of transport [*Newell et al.*, 1999] and other processes must be deduced indirectly.

[5]   (3) Regular balloon-borne ozone sensors complement campaigns (limited in time and space) and satellites (continuous but limited in vertical resolution). A network of regular ozonesonde launches records large-scale variability, stratosphere–troposphere exchange (STE), pollution layers, convective transport, seasonal and interannual variations, along with vertical structure that manifests multiple processes. Unfortunately, ozonesonde launches in the tropics have been highly sporadic, with a dozen or so stations operating intermittently since the mid-1980s. Thus, it is difficult to evaluate ozone structure and variability from observations, especially in the troposphere, and researchers using ozone profiles to develop satellite algorithms and to

evaluate model performance are faced with an inadequate database and poor statistics.

[6]   With the 1998 initiation of the Southern Hemisphere Additional Ozonesondes (SHADOZ) project, a systematic effort was made to collect regular ozone profile data at stations distributed throughout the Southern Hemisphere tropics and subtropics (sites listed in Table 2). As an augmentation of launches at operational stations, SHADOZ built on campaign efforts and infrastructure at nine sites. A tenth station joined SHADOZ in late 1998 (Irene, South Africa) and an eleventh in late 1999 (Paramaribo, Surinam). The Malindi station, on the Kenyan coast (3°S, 40°E), joined in 2001. Since 1998, SHADOZ has provided more than 1600 ozone soundings from these tropical and subtropical sites. The SHADOZ data are publicly accessible at http://croc.gsfc.nasa.gov/shadoz. The first overview of SHADOZ [*Thompson et al.*, 2002a] covered station operations and techniques, evaluated sonde precision and accuracy, and compared column ozone from the sondes with satellite data.

[7]   The present paper uses approximately 1100 SHADOZ sondes from 1998 to 2000 to characterize seasonality and variability in ozone. Specific questions addressed include:

   1. What is the seasonal and interannual variability in total and stratospheric ozone (section 3)?

   2. What is the structure of the wave-one pattern in tropical tropospheric ozone that SHADOZ stations display when data are viewed zonally? Is the wave primarily a result of tropical dynamics or photochemically produced ozone (section 4)?

   3. What is the variability in tropospheric column ozone and in lower, middle and upper tropospheric ozone layers? How do tropospheric means used in satellite and model climatologies compare to actual distributions (section 5)?

   4. Can mechanisms controlling tropospheric ozone in SHADOZ be deduced from week-to-week variability in profiles, trajectories, and other indicators of sources or

Table 2. Sites, Period of Measurements Covered, and References[a]

SHADOZ Sites	Latitude/Longitude (°)		Sampling [Reference]
Pago Pago, American Samoa	−14.23	−170.56	1995–2000 [*Oltmans et al.*, 2001]
Papeete, Tahiti	−18.00	−149.00	1995–1999 [*Oltmans et al.*, 2001]
San Cristóbal, Galapagos	−0.92	−89.60	1995–2000 [*Oltmans et al.*, 2001]
Paramaribo, Surinam	5.81	−55.2	1999–2000 [*Fortuin et al.*, 2002][b]
Natal, Brazil	−5.42	−35.38	1978–2000 [*Kirchhoff et al.*, 1991]
Ascension Island	−7.98	−14.42	1990–1992; August 1997–2000
Irene, South Africa	−25.25	28.22	1990–1993; October 1998–2000
Nairobi, Kenya	−1.27	36.80	1996–2000
La Réunion	−21.06	55.48	10/92–2000 [*Baldy et al.*, 1996]
Watukosek, Indonesia	−7.57	112.65	1993–2000 [*Fujiwara et al.*, 2000]
Suva, Fiji	−18.13	178.40	1996–2000 [*Oltmans et al.*, 2001]
Kaashidhoo, Maldives	5.0	73.5	January–March 1999 [*Lelieveld et al.*, 2001]
Aerosols99 Cruise	–	–	January to February 1999 [*Thompson et al.*, 2000]
Lusaka, Zambia, SAFARI-2000	−15.5	28	September 2000 [*Thompson et al.*, 2002b]

[a]Some stations predate SHADOZ, but this paper is based on their 1998–2000 data.
[b]J. P. F. Fortuin, et. al., Inertial instability flow in the troposphere over Suriname during the South American Monsoon, submitted to *Geophysical Research Letters*, 2002.

processes? Is there a signature of the 1997–1998 El Niño over Indian Ocean and Pacific stations (section 6)?

2. SHADOZ Network and Data

2.1. Measurements of Ozone, Temperature, and Relative Humidity

[8] Ozone measurements at SHADOZ sites (Table 2) are made with balloon-borne ECC (electrochemical concentration cell) ozonesondes coupled with a standard radiosonde and a sensor for relative humidity [*Komhyr*, 1986; *Komhyr et al.*, 1995]. At Watukosek, Java, prior to conversion to ECC sondes in August 1999, MEISEI sondes were used [*Komala et al.*, 1996; *Fujiwara et al.*, 2000; *Kobayashi and Toyama*, 1966]. Radiosondes produced by three manufacturers are used at SHADOZ stations; seven use the Vaisala manufactured sonde. Temperature is measured accurately with all radiosondes, to within 0.5–1°C. Humidity is measured with less accuracy; we use only data to −60°C although others accept data to −35°C. The nominal sampling schedule at SHADOZ stations is once per week, usually but not always midweek. Details of ozone, humidity, and temperature instrumentation for each SHADOZ station are given by *Thompson et al.* [2002a, Appendix].

[9] Because each sonde launched is essentially a new instrument, estimates of precision and accuracy in total ozone from typical sondes are required. Sonde precision, defined as the reproducibility of the total integrated ozone column, is 5% [*Thompson et al.*, 2002a]. Accuracy of integrated total ozone from the sondes, determined through comparison with rigorously calibrated ground-based total ozone instruments (R. Evans, personal communication, 2000) at five SHADOZ stations is 2–5% [*Thompson et al.*, 2002a]. The Total Ozone Mapping Spectrometer (TOMS) total ozone column, determined from a midday satellite overpass (level 2, version 7 data from the Earth-Probe TOMS instrument), is 2–4% higher than the ground-based total ozone at these stations [*Thompson et al.*, 2002a], suggesting a high-ozone bias in the TOMS observation. Using data from ten stations in the study of *Thompson et al.* [2002a], mean sonde total ozone differ-

ences with the column determined from TOMS satellite overpasses range from 2% to 11%, when total ozone is computed with an above-balloon burst extrapolation from solar backscattered ultraviolet (SBUV). Discrepancies between total ozone determined from sondes and from satellite evidently arise from the stratospheric as well as tropospheric part of the sonde profile [*Thompson et al.*, 2002a]. In the following sections, analyses are based on features at individual stations and/or seasonal averages for which station-to-station biases in ozone amounts have no impact.

[10] Closer examination of sonde-TOMS and sonde-Dobson offsets in total ozone suggests station-to-station biases among SHADOZ stations [*Thompson et al.*, 2002a] due to differences in sonde technique [*Johnson et al.*, 2002]. Data processing, sensor solution and hardware vary, even though the same basic instrument is used at all sites. The relationship of individual station offsets to technical details is not entirely clear. There are no significant differences in mean integrated column amount in the lower stratosphere [*Thompson et al.*, 2002a] although there is some evidence that higher upper stratospheric ozone at Nairobi (Figure 2) relative to the other stations might be an instrumental effect. The various sonde techniques used at SHADOZ stations are being evaluated through comparison with test chamber results that simulated tropical ozone profiles (Juelich Ozonesonde Intercomparison Experiment, JOSIE-2000, www.fz-juelich.de/icg/icg2/forschung/Josie).

2.2. Data Selection and Treatment

[11] The 1998–2000 data used in this study are taken from the SHADOZ website and are also available from the World Ozone and Ultraviolet Data Center (WOUDC) in Toronto (http://msc-smc.ec.go.ca/woudc). Coordinates for each SHADOZ station are summarized in Table 2, along with those for four campaign data sets that reside in the archive. Aerosols99 data were taken between 30N and 30S from the R/V *Ronald H. Brown* oceanographic vessel as described by *Thompson et al.* [2000]. The INDOEX data were taken in January–March 1999 from the Kaashidhoo Observatory at Male in the Maldives. During the SAFARI-2000 experiment [*Swap et al.*, 2002] in September 2000,
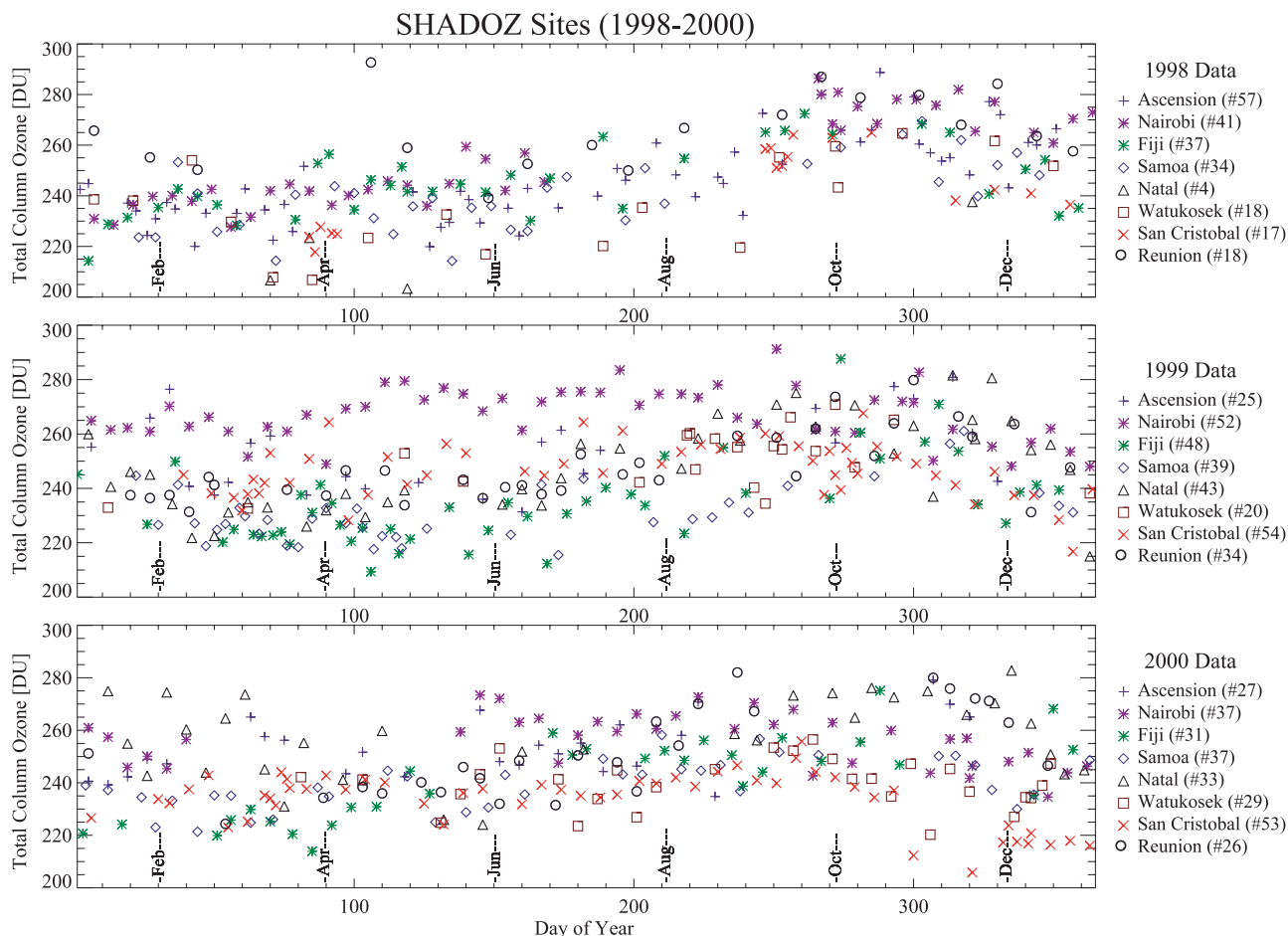
Figure 1. Time series of total column ozone (DU) for eight SHADOZ stations for 1998 (upper), 1999 (middle), and 2000 (lower). Station and sample number are indicated to the right. Total ozone calculations use the SBUV extrapolation from 7 hPa or balloon burst to the top of the atmosphere.

ozonesonde launches were made in Lusaka, Zambia [*Thompson et al.*, 2002b].

[12] Total ozone in each SHADOZ data record (as used here) is based on integration to 7 hPa or balloon burst (whichever is higher), with extrapolation to 1 hPa based on the SBUV satellite climatology of *McPeters et al.* [1997]. No normalization is made to total ozone from another instrument, i.e., satellite or a ground-based total ozone sensor. The difference between total ozone computed with an SBUV extrapolation may be up to 8% lower than using a constant mixing ratio approach [*McPeters et al.*, 1997; *Johnson et al.*, 2002; *Thompson et al.*, 2002a]. The SHADOZ website includes 5-day back-trajectories initialized from the station coordinates at 12Z on the day of launch. A kinematic version of the Goddard trajectory model [*Schoeberl and Newman*, 1995] is used to track air parcels starting at 750, 500, 300, and 200 hPa. The wind fields are taken from the NCEP reanalysis [*Kalnay et al.*, 1996].

[13] Tropospheric ozone is determined by integration to a "chemical tropopause," which is defined as the point at which extrapolation of the lower stratospheric ozone mixing ratio reaches 100 ppbv ozone. This is within 10–15 hPa of the temperature-based tropopause (e.g., as supplied by NCEP) except at Irene, where the temperature sometimes shows a double tropopause. Stratospheric ozone column amounts are determined by integration from the chemical tropopause to balloon burst with extrapolation as described above.

3. Total and Stratospheric Ozone and Quasi-Biennial Oscillation (QBO)

[14] Figure 1 shows total ozone at eight SHADOZ sites in separate panels for 1998, 1999, and 2000. Figure 2 shows stratospheric ozone at the same sites. Previous studies of ozone at some of these stations [*Logan and Kirchhoff*, 1986; *Kirchhoff et al.*, 1996; *Olson et al.*, 1996; *Thompson et al.*, 1996a, 1996b; *Oltmans et al.*, 2001; *Taupin et al.*, 1999; *Logan*, 1999a, 1999b; *Fujiwara et al.*, 2000] show that a typical pattern is a period of highest total (and highest stratospheric) ozone in the August–November period. For the sites operational in the early to middle 1990s (all except Nairobi and San Cristóbal), the same pattern occurred during 1998–2000. Seasonal mean differences for total ozone range from 9 to 30 DU (Table 3), depending on site. Except for San Cristóbal and Nairobi the typical stratospheric seasonal column difference is 11–20 DU (Table 3). Less than 5 DU of this difference is due to the tropopause being lower in SON than in MAM. The tropopause is normally between 16 and 18 km except for Réunion and
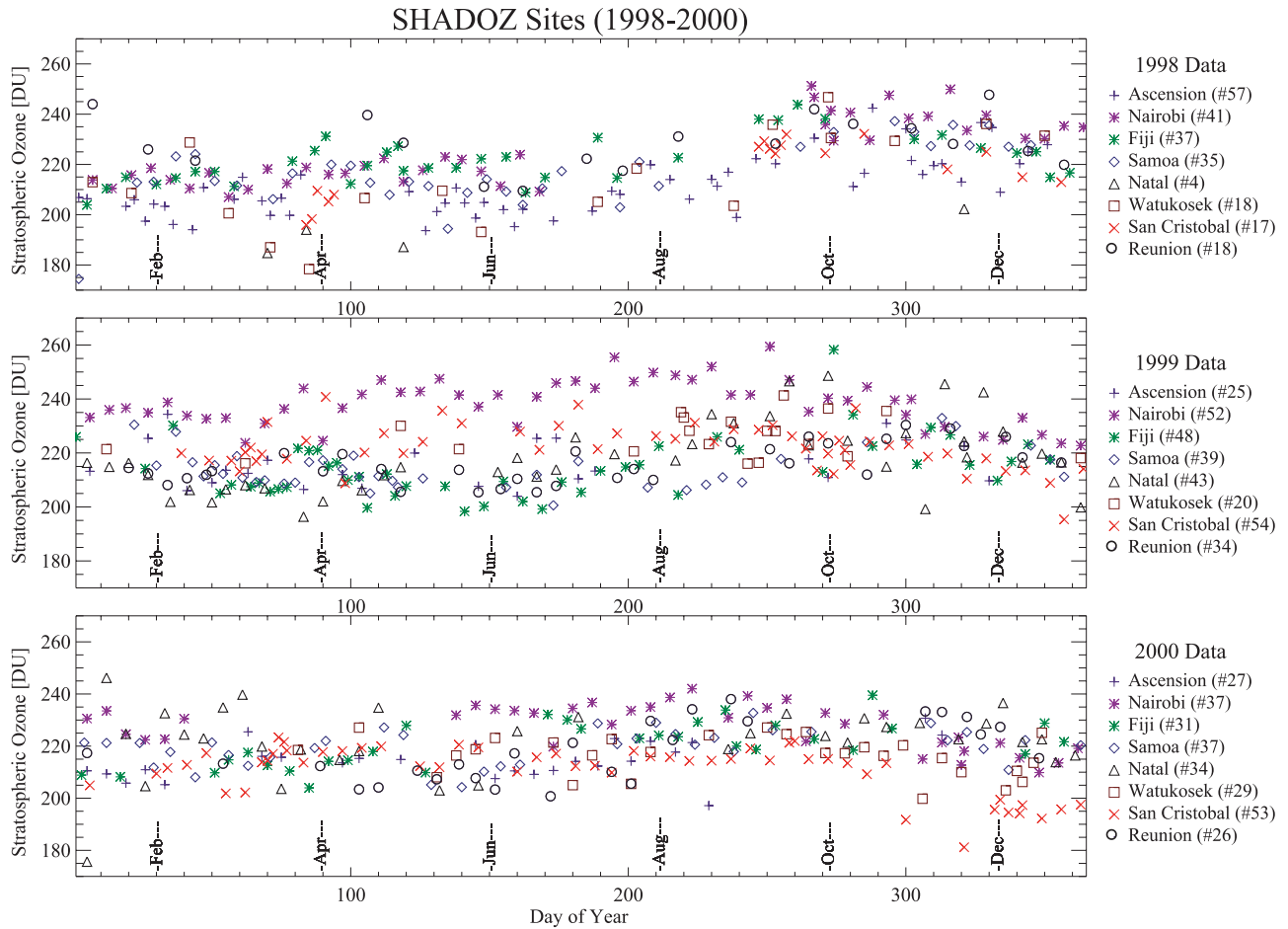
SHADOZ Sites (1998-2000)

Figure 2. As Figure 1, except for stratospheric column ozone (DU). Values are determined by integration from the tropopause (determined by ozone gradient, see text) to 7 hPa or burst with SBUV extrapolation.

Irene, where the tropopause sometimes falls below 14 km [*Chane-Ming et al.*, 2000].

[15] Interannual variability in total column ozone over the equator is dominated by the QBO [e.g., *Bowman*, 1989; *Hollandsworth et al.*, 1995; *Bojkov and Fioletov*, 1996; *Thompson et al.*, 1996b]. The QBO is a downward propagating oscillation between easterly and westerly wind regimes in the equatorial stratosphere, with a period of

Table 3. Summary of Integrated Column Amounts From 1998–2000 SHADOZ Data and Associated Campaigns[a]

Site	Total Mean (1σ)			Stratospheric Mean (1σ)		Tropospheric Mean (1σ)		
	SN	MAM	SON	MAM	SON	SN	MAM	SON
Samoa	35/19	229 (8)	252 (9)	212 (6)	229 (6)	41/24	16 (5)	23 (5)
Tahiti	24/17	226 (7)	257 (6)	208 (7)	230 (8)	26/17	17 (4)	27 (4)
San Cristóbal	38/41	237 (14)	246 (14)	216 (13)	219 (11)	38/41	21 (3)	27 (4)
Natal	20/22	235 (16)	269 (14)	209 (14)	227 (13)	20/22	26 (5)	41 (6)
Ascension	29/29	242 (12)	263 (16)	210 (7)	220 (12)	29/30	33 (7)	43 (7)
Nairobi	29/38	257 (15)	266 (13)	228 (12)	235 (10)	29/40	29 (6)	31 (6)
Irene	13/22	254 (11)	284 (9)	224 (11)	248 (9)	13/23	30 (6)	38 (7)
Réunion	18/20	243 (14)	270 (11)	213 (9)	229 (8)	21/22	29 (7)	41 (5)
Watukosek	14/23	233 (15)	247 (11)	211 (15)	222 (10)	19/25	20 (5)	25 (6)
Fiji	35/24	233 (11)	260 (18)	215 (8)	231 (15)	35/25	18 (6)	28 (8)
		Campaigns						
		Total Mean (1σ)	Stratospheric Mean (1σ)	Tropospheric Mean (1σ)				
Aerosols99	12	252 (14)	214 (12)	37 (3)				
INDOEX	48	246 (9)	218 (8)	29 (5)				

[a]SN = number of samples, 1-sigma is standard deviation from mean. Total and stratospheric ozone obtained with SBUV climatological extrapolation [*Thompson et al.*, 2002a]. Tropospheric ozone from integration of sonde. All in Dobson units. Station data from March–May (MAM) and September–November (SON) sets.
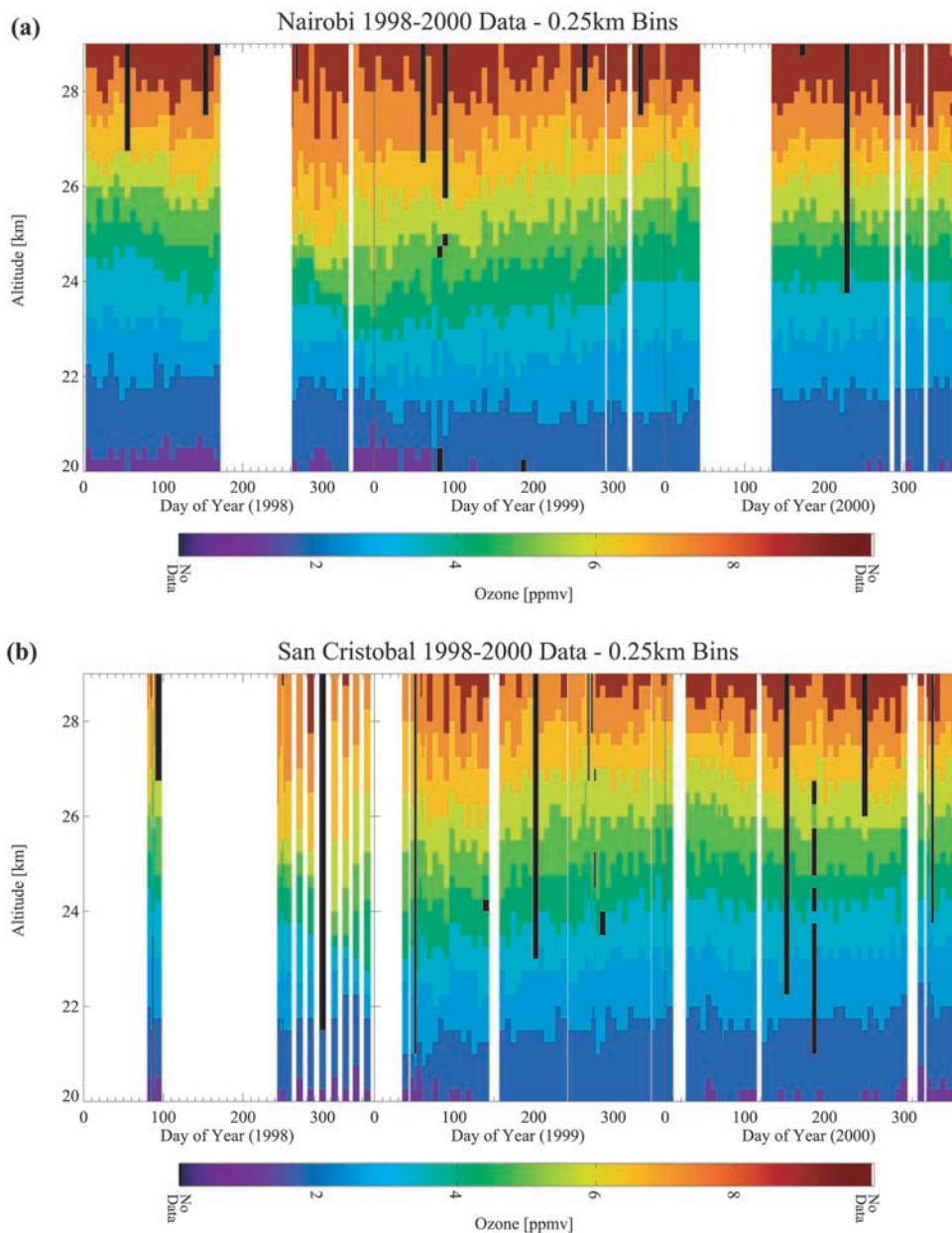
Figure 3. Time versus altitude stratospheric ozone mixing ratio (in ppmv) is based on 0.25 km profile averages for (a) Nairobi and (b) San Cristóbal.

about 28 months [*Reed*, 1964; *Baldwin et al.*, 2001]. The 1998–2000 SHADOZ data cover a complete cycle of the QBO (J. A. Logan et al., The quasi-biennial oscillation in equatorial ozone as revealed by ozonesonde and satellite data, submitted to *Journal of Geophysical Research*, 2002, hereinafter referred to as Logan et al., submitted manuscript, 2002). The winds above ∼30 hPa (24 km) are easterly in the first half of 1998, and the westerly shear zone descends from near 10 hPa in mid-1998 to ∼35 hPa by the end of 1998. The westerlies continue during 1999 at 20 hPa, and the next easterly shear zone descends through 10 hPa at the middle of 1999. The winds become westerly at 10 hPa in December 2000. The descending westerly shear zone in middle to late 1998 leads to a large increase in the stratospheric column that is evident in the sondes over most

stations (Figure 3) and the TOMS overpass data [*Thompson et al.*, 2002a, Figure 6]. There is a gap in some sonde records prior to September 1998 (e.g., Nairobi and San Cristóbal) (Figures 3a and 3b) but the sonde data clearly mimic the TOMS variations. The SHADOZ data for Nairobi, Ascension (not shown) and San Cristóbal are the first in situ data to document the change in shape of the equatorial ozone profile from 17 to 34 km (Logan et al., submitted manuscript, 2002). During 1998, the QBO signal reinforces the seasonal cycle, leading to an increase in ozone from August to November. Ozone partial pressures at Nairobi exceed 15 mPa at 26 km (or 6–7 ppmv) (Figure 3a) from September 1998 to May 1999.

[16] Analyses of column and Stratospheric Aerosols and Gases Experiment (SAGE) profile data have shown that the

QBO in ozone is strongest over the equator [*Bowman*, 1989; *Hollandsworth et al.*, 1995; *Zawodny and McCormick*, 1991; *Hasebe*, 1994; *Randel and Wu*, 1996]. The column ozone variations within 10° of the equator are approximately in phase with the equatorial winds near 30 hPa, whereas the extratropical variations are of opposite phase, with the phase change near 10°–15° of the equator. The QBO signal while less distinct in the stratospheric data for Samoa, Fiji, and Tahiti (Figure 2) because of the change in phase, is still present at the same altitudes as at Nairobi and San Cristóbal. A full analysis of the QBO using the SHADOZ data record is given by Logan et al. (submitted manuscript, 2002).

4. The Zonal Wave-One in Tropospheric Ozone

4.1. Summary of Column-Integrated Ozone: Wave-One

[17] A number of studies have attempted to determine whether the equatorial wave-one pattern in total ozone seen in satellite data [*Shiotani*, 1992] is in the troposphere, the stratosphere or both. Satellite data are inconclusive because they are at poorest precision in the region (70–100 hPa) where the stratospheric wave is expected [*Newchurch et al.*, 2001]. Although sondes resolve the vertical structure with the required resolution, prior to SHADOZ, a complete zonal view was lacking due to temporal and spatial gaps. The statistics in Table 3 show evidence of a "tropospheric wave-one," with tropospheric ozone column amounts at Natal, Ascension, Nairobi (and Réunion) usually higher than at Watukosek, Fiji, Samoa and Tahiti. A wave-one is also apparent when TOMS total ozone at these stations (and Dobson where applicable) are contrasted [*Thompson et al.*, 2002a]. *Thompson et al.* [2002a, Table 5] show total, stratospheric, and tropospheric ozone averaged over the sets of four stations and estimates the magnitude of the wave obtained by subtracting the two quantities. Even given fairly high standard deviations, total ozone and tropospheric ozone show 10–15 DU wave-one amplitudes at all times of year. Stratospheric ozone shows no statistically significant wave [*Thompson et al.*, 2002a, Figures 12–14] on average, although a small wave cannot be ruled out due to instrument variability. Lower stratospheric ozone is uniform at all SHADOZ stations except Irene, which is higher because of its frequent midlatitude character.

4.2. Structure of the Tropospheric Ozone Wave-One

[18] The wave-one in tropospheric ozone is evident when seasonally averaged data are displayed zonally (Figures 4a and 4b). Longitudinal cross sections in December–February and June–August (not shown) confirm that the wave persists throughout the year. Between 40°W (just west of Natal) and ~60°E, enriched midtropospheric ozone gives rise to the wave-one. Regions with greater than 80 ppbv ozone (brown) appear at lower altitudes over the Atlantic, Africa and the western Indian Ocean than over the Pacific and eastern Indian Ocean. This tendency is prominent in SON when ozone subsidence maximizes over the Atlantic [*Krishnamurti et al.*, 1996]. Free tropospheric ozone mixing ratios >60 ppbv over the Atlantic have been observed with aircraft, balloon and shipboard soundings taken in months from September to June [*Smit et al.*, 1989; *Browell et al.*,

1996; *Weller et al.*, 1996; *Thompson et al.*, 1996a, 2000]. Advected ozone and ozone precursors from pollution recirculate and enrich tropospheric ozone in both MAM and SON (Figure 4). A significant amount of ozone in SON may form from NO created by lightning [*Moxim and Levy*, 2000; *Martin et al.*, 2000]. Ozone near the surface is much lower than in the midtroposphere (except for Watukosek in SON) because SHADOZ sites are generally far from regions polluted in ozone and rich with ozone precursors. In contrast, during SAFARI-2000 (September 2000), surface ozone at Lusaka, Zambia, in the heart of active African fires, was 55–95 ppbv [*Thompson et al.*, 2002b].

[19] In MAM (Figure 4a), the tropopause is higher than 16 km (steep ozone gradients, tight contours) over all stations; it appears to be 1–3 km lower in SON (Figure 4b). The ozone distribution in Figure 4 reflects typical large-scale tropical circulation, returning to normal conditions following the 1997 El Niño–Southern Oscillation (ENSO). Subsidence occurs over the Atlantic and adjacent continents. Intense convection occurs mostly over the eastern Indian Ocean, Indonesian maritime continent, and the Pacific. Because these locations are usually remote from sources, the local effect on ozone tends to be reduction of the ozone column as ozone-rich air in the middle to upper troposphere is displaced by ozone-poor air from the surface. In MAM, ozone averaging <20 ppbv extends from the surface to 3 km over the western Pacific (Fiji–Samoa–Tahiti). In the same region, an ozone minimum (20 ppbv contour) also extends from 8 to 13 km (Figure 4a). The convective character of this region has been pointed out by *Folkins et al.* [1999, 2000, 2002] [see *Pickering et al.*, 2001] for a case study of convective impact on ozone near Fiji in March 1999.

[20] In SON (Figure 4b), the upper tropospheric convective signature in ozone is most prominent over Watukosek. There is also higher ozone near the surface, presumably from aged pollution [*Fujiwara et al.*, 2000; *Thompson et al.*, 2001]; low ozone in this region occurs at 9–14 km. Over the central Pacific, surface ozone concentrations in SON are higher than in MAM but still appear as regional minima, mixed throughout the lower troposphere and up to 10–12 km. Upper tropospheric descent over the western Indian Ocean to Atlantic (40°W–70°E) is more apparent in ozone for SON than MAM, as indicated by the 70–80 ppbv contours.

5. Variability in Tropospheric Ozone: Column, Layers, and Profiles

[21] The most striking feature of tropospheric ozone at the SHADOZ stations is considerable temporal and regional variability. Indeed, SHADOZ profiles show more seasonal and meteorological variability than data from some midlatitude stations (e.g., Lauder, New Zealand and Hohenpeissenberg, Germany). Only the San Cristóbal and Nairobi stations display less than a factor of 3 difference in tropospheric ozone column amounts within a calendar year (Figure 5). This makes interpretation and evaluation of ozone budgets and preparation of meaningful climatologies for models and satellite retrievals a challenge. In this section, we show that the best statistical approaches are not based on simple averages or composites of the data. In
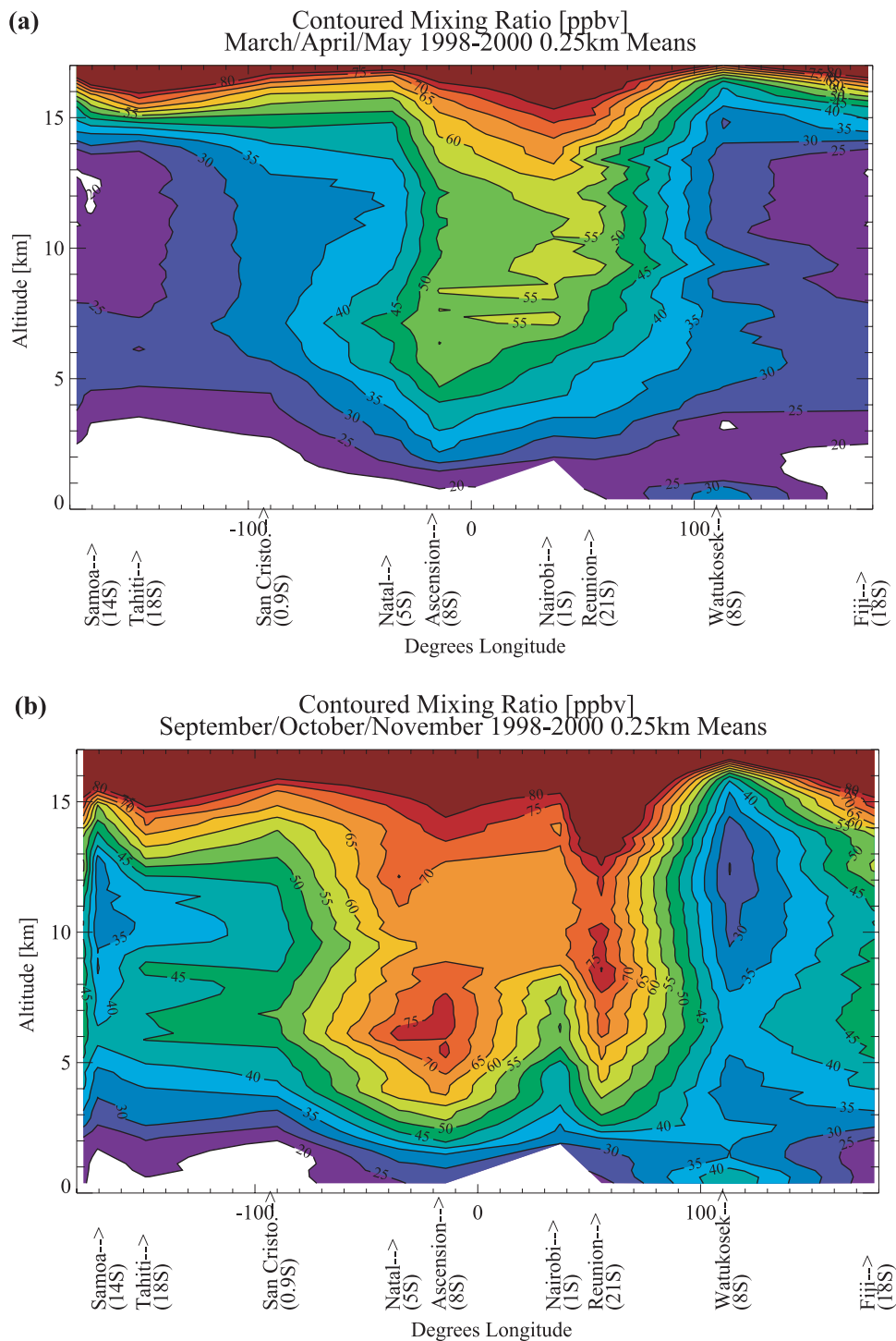
(a)

Contoured Mixing Ratio [ppbv]
March/April/May 1998-2000 0.25km Means

(b)

Contoured Mixing Ratio [ppbv]
September/October/November 1998-2000 0.25km Means

Figure 4. Contoured ozone mixing ratio (ppbv) for (a) MAM 1998–2000 months. Station locations (latitude in brackets) are indicated below. Calculations are based on 0.25-km mean profiles at each station for those months. (b) Same as (a), except analyses for SON months.

order to quantify ozone budgets and to forecast pollution, models must be able to reproduce these features with realistic simulations of sources, chemical and transport processes.

[22] In section 6, we examine processes contributing to week-to-week ozone variability at representative SHADOZ stations. In the following sections, we discuss:

1. Column amounts and means within layers (section 5.1).
2. SHADOZ profiles and the tropical profile used in the TOMS v. 7 algorithm (section 5.2).

5.1. Column and Layer Variability

[23] In general at SHADOZ sites, tropospheric ozone column amounts (Figure 5) are greater between June and
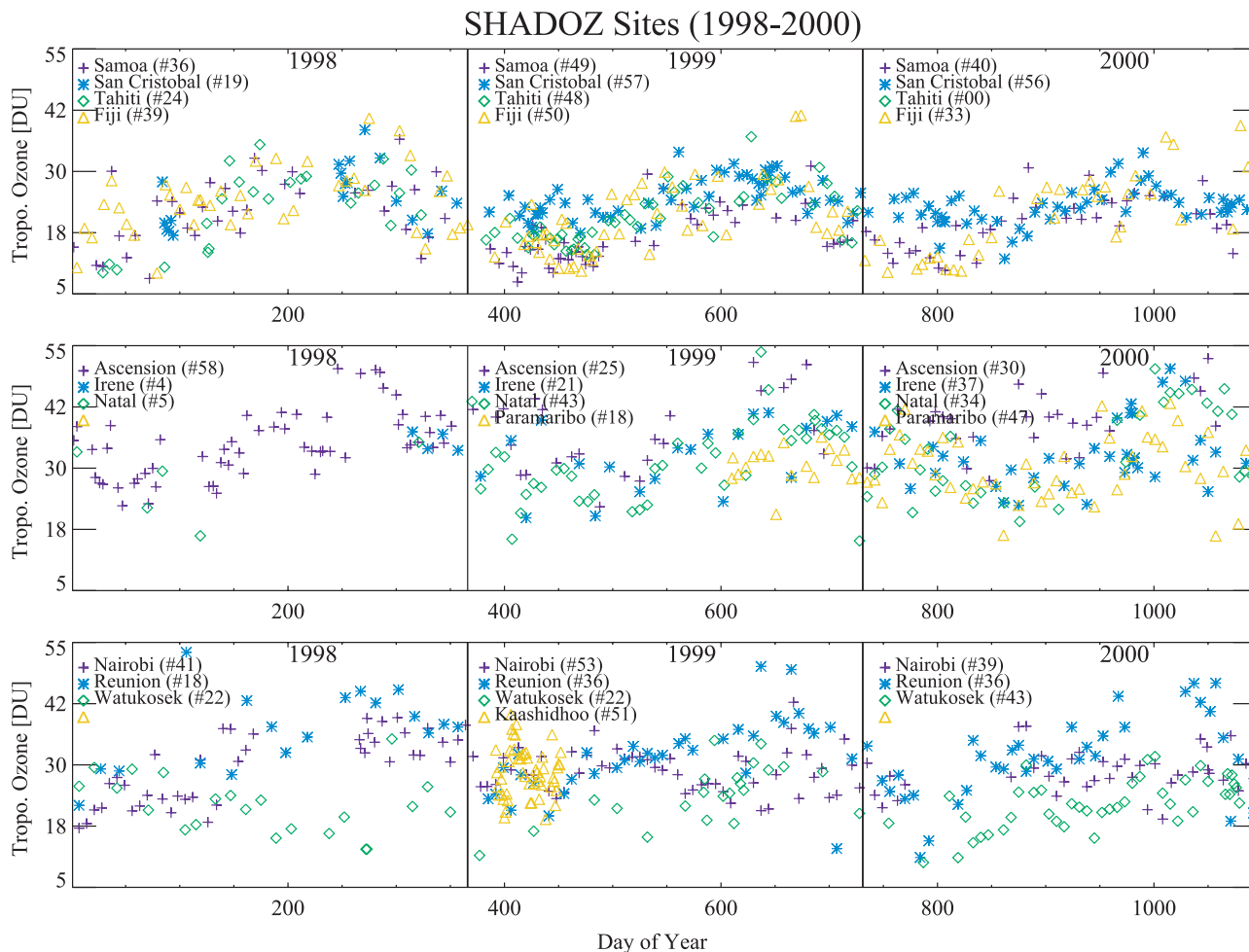
SHADOZ Sites (1998-2000)

Figure 5. Tropospheric ozone column from sondes (in DU) 1998–2000. Top panel: Pacific sites (Samoa, San Cristóbal, Tahiti, and Fiji). Middle panel: Atlantic stations (Natal, Ascension, and Paramaribo) and Irene. Bottom panel: Indian Ocean stations (Réunion and Watukosek) and Nairobi with Kaashidhoo INDOEX campaign data shown for early 1999.

November than at other times of year. This is also the period of greatest week-to-week change at the most variable stations: Fiji, Ascension, Natal, Nairobi, and Réunion. Depending on the station and the year, Figure 5 shows that minimum ozone usually occurs between January and May and that each station has a characteristic minimum ozone amount. For example, a number of soundings with 10 DU ozone or less appear at Samoa and Fiji in early 1999 (Figure 5, upper panel) during the PEM-Tropics B field campaign [*Oltmans et al.*, 2001]. At Ascension and Irene, the minimum lies between 20 and 25 DU; it is 5 DU lower at Natal and Paramaribo (Figure 5, middle panel). Tropospheric ozone column amounts and variability at Watukosek (Figure 5, lowest panel) are generally similar to the Pacific stations.

[24] The SHADOZ variability indicates that a significant level of information is lost when monthly or seasonally averaged sonde parameters are used, which is often the case in comparisons with model or satellite-derived quantities [e.g., *Martin et al.*, 2002]. The variability of individual column amounts at SHADOZ stations over the course of a year, a factor of 3 for 8 of 10 stations, is reduced to a factor of 2 or less when monthly averages are taken.

Within individual layers, e.g., mean mixing ratios in the 5–10 km layer (triangles in Figure 6), the annual variability is a factor of 5 at Fiji and Réunion. Within a given season, for example, in SON when the stratospheric column ozone is almost invariant (Table 3), tropospheric ozone is highly variable, a factor of 2.5 for individual layers within a week or two (Figure 6c, Fiji). Campaigns show that changes of this magnitude can occur on 1–2 day timescales. Figure 6 shows that the greatest variability occurs in the middle and upper tropospheric layers. In the latter case, some stratospheric influence may be operating. Midtropospheric ozone is most affected by variations on synoptic scale, e.g., long-range transport, biomass burning, and convection (section 6).

[25] Figure 7 shows histograms for the mean mixing ratio in the lower (0–5 km), middle (5–10 km) and upper (10–15 km) layers in SON. Two results are most noteworthy. First, there are significant differences in distributions among stations for which mean column amounts and/or profiles are similar, e.g., Ascension, Natal, Réunion (Figures 7a–7c). It is therefore inappropriate to use data from these sites interchangeably. At 10–15 km, there is a greater predominance of high values at Réunion relative to the other two
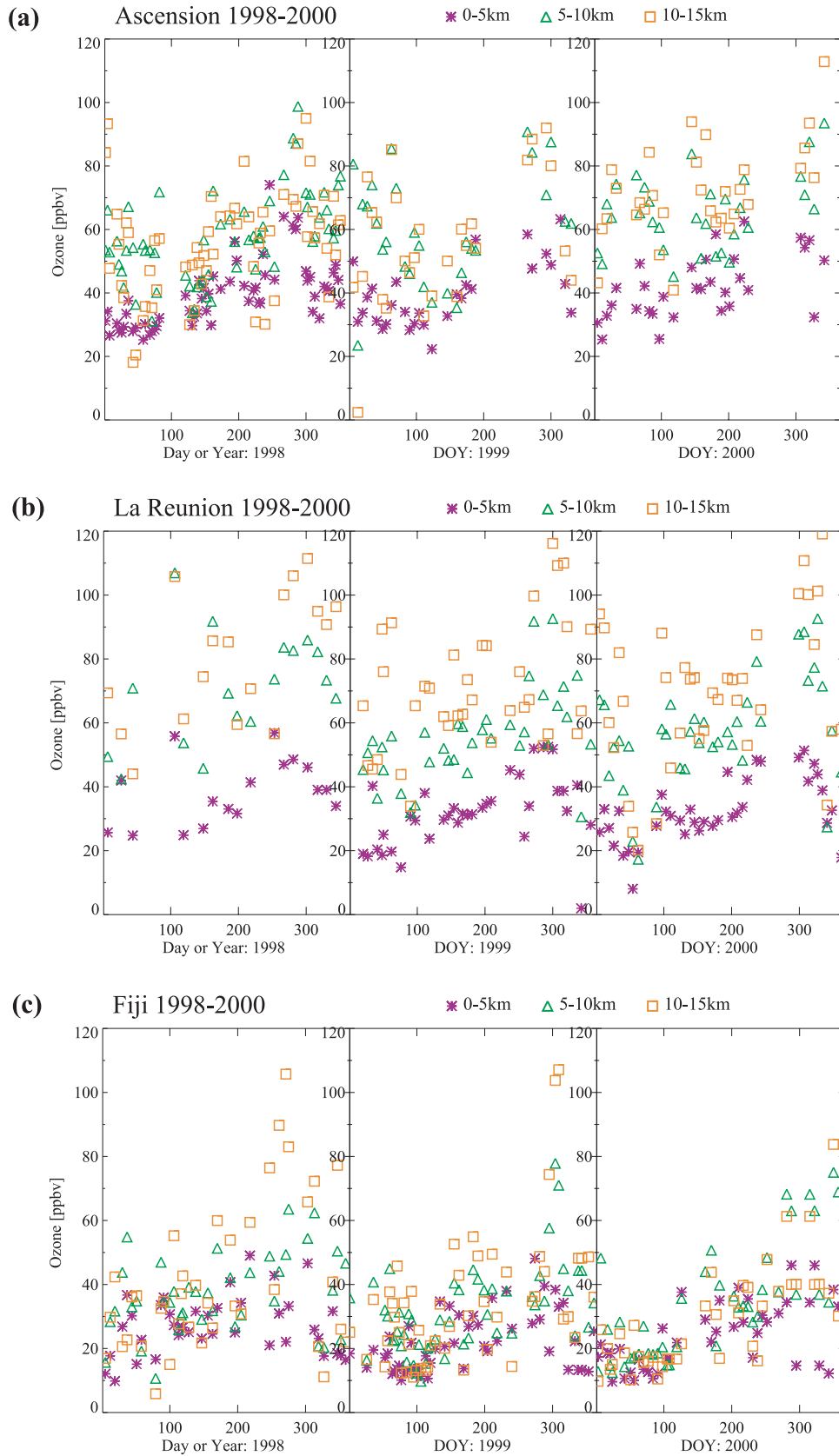
Figure 6. Variability in layers. Mean mixing ratios in 0–5, 5–10, and 10–15 km segments from sondes at (a) Ascension, (b) Réunion, and (c) Fiji.
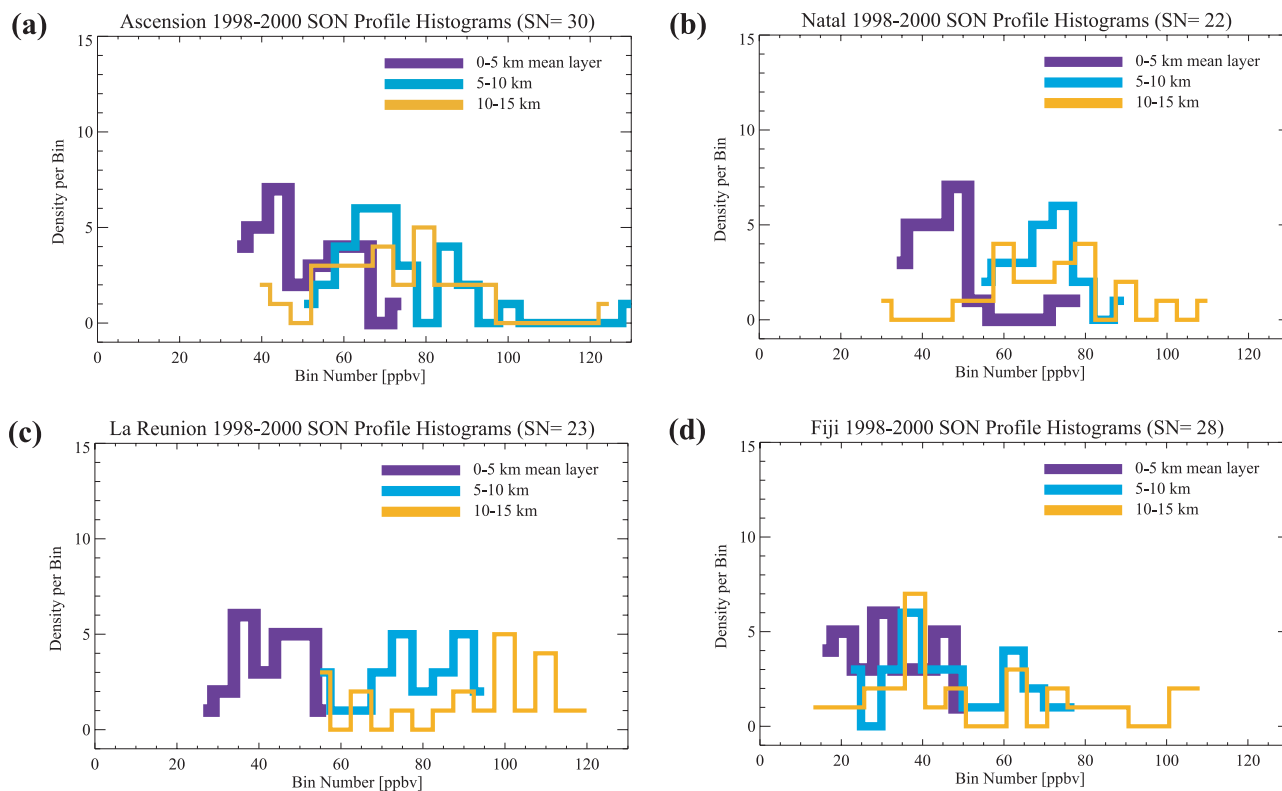
Figure 7.   Histograms of mean ozone mixing ratio (ppbv) within 5 km layers for SON. Designations 0–5 km (purple), 5–10 km (blue), 10–15 km (yellow). Sample number (SN) given. (a) Ascension, (b) Natal, (c) Réunion, and (d) Fiji.

stations. In the lowest levels (0–5 km) Ascension has a large cluster of values >60 ppbv, which is not the case for Natal and Réunion. Second, averaged amounts within each layer often fall at a minimum in the distribution. At Ascension and Fiji (Figure 7d), the 5–10 km mean lies near a minimum in the distribution (near 90 and 45 ppbv, respectively). Using simple averages from the sondes is risky; selected values may rarely occur and thus have little physical significance. A recent study of ozone profiles from aircraft landings and takeoffs near Irene (R. D. Diab et al., Classification of tropospheric ozone profiles over Johannesburg based on MOZAIC aircraft data, submitted to *Atmospheric Chemistry and Physics*, 2002) shows that distinct profiles correspond to varying synoptic situations.

5.2. Tropospheric Ozone Profiles for Satellite Climatology

[26]   A primary motivation for SHADOZ is to improve the ozone profile climatology used in satellite ozone retrievals. Tropical profiles currently used in the TOMS algorithm use several values of total ozone with stratospheric variations but almost no difference in the troposphere (below 100 hPa). For example, a standard profile based on 225 DU total ozone assumes a tropospheric ozone column amount (1000–100 hPa) of 29.8 DU; the 275 DU profile is 31.0 DU. Both profiles are 14.6 DU from the surface to 500 hPa. However, the SHADOZ climatology shows that individual tropospheric column ozone amounts are highly variable, ranging between 10 and 50 DU (Figure 5) with seasonally averaged extremes of 16 DU (Samoa in MAM) (Table 3)

and 43 DU (Ascension in SON). The standard profile for a TOMS tropical ozone column of 250 DU (tropospheric section only), obtained by averaging the 225 and 275 DU profiles, is the black line in each panel of Figure 8. The MAM and SON 0.25 km means are indicated in blue and red, respectively (1-sigma standard deviation in shaded gray). Some mean profiles agree with the standard profile very well, e.g., Ascension (MAM) (Figure 8a) and Fiji (SON) (Figure 8b). Samoa (Figure 8c) has the overall poorest agreement.

[27]   The most serious divergence from the standard profile is below 500 hPa. This is the point at which the retrieval efficiency drops off rapidly over low reflectivity (0.1–0.3) surfaces [*Klenk et al.*, 1982]. For the satellite at nadir, the efficiency with which ozone is measured at 1000 hPa is only 25% when the reflectivity is 0.1 [*Hudson et al.*, 1995, Figure 2]. Because all SHADOZ stations are relatively remote from ozone sources (relatively small discrepancy with the standard unpolluted profile at 1000–800 hPa), the mean profiles at the sites with greatest pollution (Ascension, Natal, Réunion) do not give large deviations from the TOMS climatology. A different picture emerges from the mean of 9 profiles taken at Lusaka, Zambia in September 2000 (Figure 8d). Located in the midst of central African biomass burning, at least 30% of Lusaka's surface ozone is due to local pollution. Most pollution layers reaching up to 200 hPa are imported from neighboring countries [*Thompson et al.*, 2002b].

[28]   Table 4 summarizes the mean column amount for the MAM and SON profiles to 100 hPa and 500 hPa. If it is
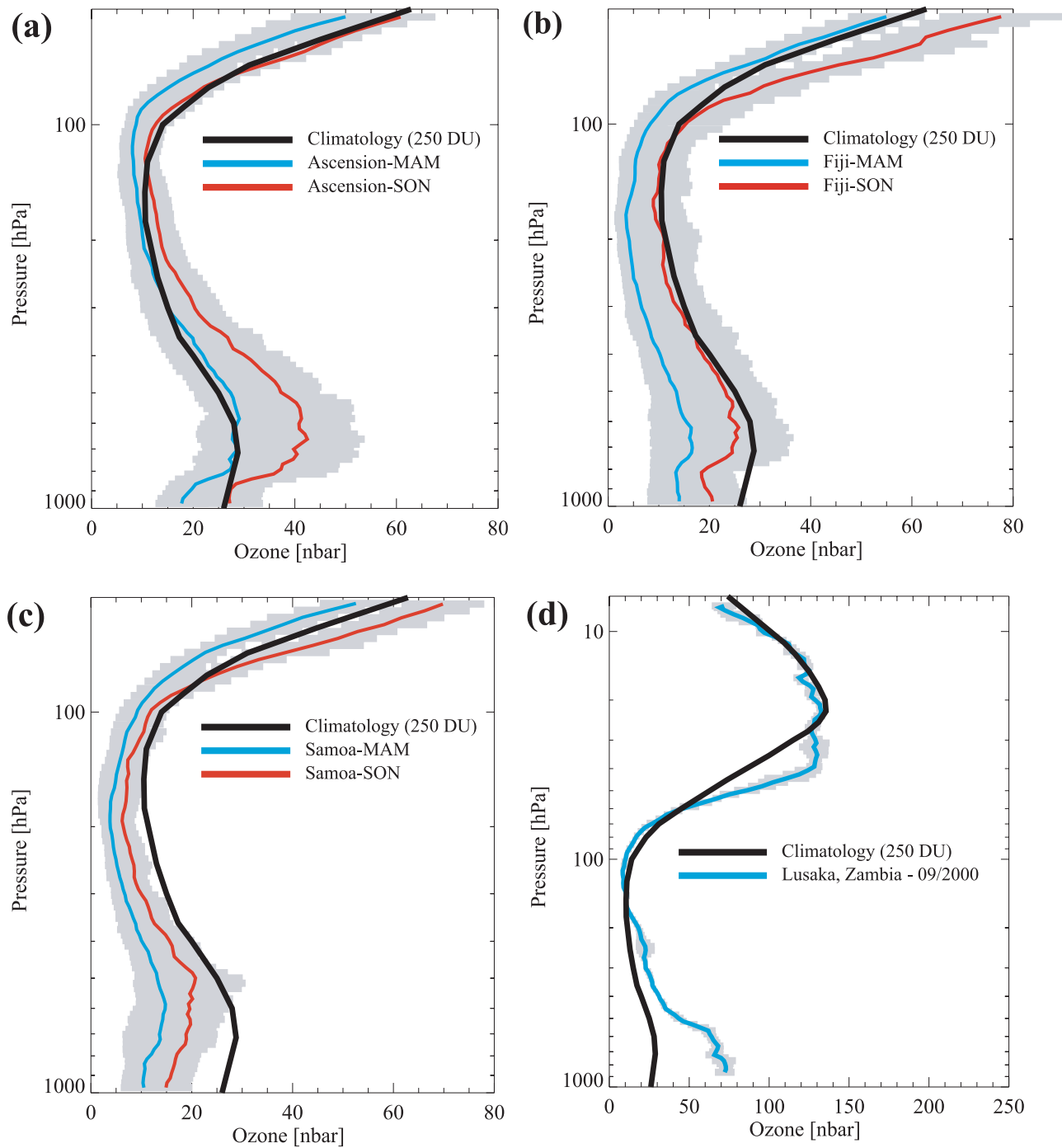
Figure 8. TOMS 250 DU climatological profile (black) with seasonally averaged profiles for MAM (blue) and SON (red) based on 1998–2000 SHADOZ data. (a) Ascension, (b) Fiji, and (c) Samoa. (d) From a 9-sonde average collected from 6 to 11 September 2000 over Lusaka, Zambia [*Thompson et al.*, 2002b].

assumed that the satellite retrieval down to 500 hPa is accurate, then the average potential error is estimated as the difference between the seasonal mean column amounts and the climatology when the latter is greater than actual. In other words, at Samoa in MAM the mean overestimate is 8.0 DU. This is ∼50% of the tropospheric column or 2.8% of a total 225 DU ozone column. At stations for which the actual ozone exceeds climatology, 65% is assumed to be an

estimate of retrieval efficiency of the difference. At Ascension in SON, for example, (42.7 − 29.8 DU) × 0.65 = 8.5 DU would be added to 29.8 DU (38.3 DU) in the measurement. This is ∼10% lower than actual tropospheric ozone and represents a 2% error in the total column. For Lusaka (Figure 8d), several profiles were 54 DU; the tropospheric underestimate is >15%. Approximately one-third of the ozone profiles lie outside the shaded range Figures 8a–8c.

Table 4. Column-Integrated Ozone for TOMS Standard Profile and Seasonal Means From SHADOZ (1998–2000) Data (as in Figure 8)

Station	Surf to 100 hPa, MAM	Surf to 100 hPa, SON	Surf to 500 hPa, MAM	Surf to 500 hPa, SON
TOMS, 225 DU	29.8 DU	29.8 DU	14.6	14.6
Ascension	30.7	42.7	13.0	18.6
Natal	24.2	40.3	10.5	17.0
Réunion	28.2	42.3	10.8	16.0
Fiji	15.9	28.4	7.7	11.3
Samoa	15.2	22.3	6.7	9.1

For example, during SON, the mean mixing ratio for Ascension in the 0–5 km layer is 50 ppbv; this represents an average between two peaks at 40 ppbv and 60 ppbv. The latter value is about a factor of 1.5 greater than the standard profile and the potential ozone retrieval error is greater than that based on the mean.

6. Tropospheric Ozone Variability in the SHADOZ (1998–2000) Period

[29] Tropospheric ozone data from the 1998–2000 SHADOZ record are used to address the following:

1. What is the general seasonal and interannual variability seen in tropospheric ozone among SHADOZ sites? Are there signatures of the waning ENSO in the early SHADOZ record? (section 6.1)

2. Can episodes of convection, pollution transport and upper tropospheric or lower stratospheric ozone exchange be observed in 1998–2000 (section 6.2)?

3. What appear to be general influences on tropospheric ozone at SHADOZ stations, e.g., origins of free tropospheric air, biomass burning? (section 6.3).

6.1. General Seasonal and Station Variability: ENSO

[30] On average, as noted in section 4, tropospheric ozone during 1998–2000 reflected normal or "unperturbed" tropical circulation although the SHADOZ record started during the latter stages of the 1997–1998 ENSO. Modified convection patterns associated with the ENSO tend to perturb column ozone amounts [*Shiotani*, 1992]. Ozone over the central and eastern Pacific decreases as convection brings low surface ozone up through the troposphere.

[31] The strongest ENSO of the last century included the first few months of SHADOZ. In March 1997, tropospheric ozone column depth from Africa to the maritime continent increased more than 20 DU as a result of the strong ENSO and a warming of the Indian Ocean associated with a temperature distribution called the Indian Ocean Dipole [*Saji et al.*, 1999; *Webster et al.*, 1999]. The ENSO and Indian Ocean Dipole increased subsidence over the maritime continent, leading to drought and forest fires in Indonesia. Smoke and tropospheric ozone pollution from the fires spread rapidly to other southeast Asian countries and westward toward India [*Thompson et al.*, 2001]. The ENSO and Dipole effects peaked in October and November 1997 and reversed sign when the ENSO switched to the La Niña phase in 1998. At the transition elevated ozone was detected over Fiji (Figure 5, top panel) and Watukosek (bottom panel). Although the Watukosek soundings (25–28 DU in early 1998) are much less than the 55 DU recorded in October 1997 [*Fujiwara et al.*, 1999], these values are

greater than normal (compare January–March 1999 and 2000 in Figure 5) [see *Komala et al.*, 1996].

[32] In the second panel of Figure 5, Natal and Ascension appear similar to one another although the data are somewhat sparse in 1998. These stations, along with Réunion, have the highest tropospheric ozone column and the greatest sonde-to-sonde variability. Where coincident data are available from all SHADOZ sites, Ascension tends to be highest in tropospheric ozone (Figure 5, middle panel). An exception occurred in April 1999 when a column of ~20 DU was recorded at Ascension and Natal. Early 1998 tropospheric ozone total at Ascension is much lower than for the same period in 1999 and 2000 (note soundings <30 DU), possibly an anomaly associated with the waning ENSO. Except for April and May, soundings with >40 DU of tropospheric ozone have been recorded in every month at Ascension.

[33] At Réunion (Figure 5, lowest panel), there appear to be two ozone maxima, one in April–June, possibly from central African burning in the early part of the dry season. Pollution in SON from more southerly Africa and Madagascar biomass fires has been well studied [*Baldy et al.*, 1996; *Taupin et al.*, 1999, and references therein]. Fiji (Figure 5, top) also displays two periods of elevated ozone in 1999 and 2000. The influence of African fires is usually greatest in Fiji after August [*Oltmans et al.*, 2001]. At Fiji, there occurs some of the lowest upper troposphere (UT) ozone seen in the SHADOZ record. Fiji's proximity to the South Pacific Convergence Zone (SPCZ) brings unpolluted marine air to the upper troposphere. Nairobi's tropospheric ozone column (Figure 5, bottom) is relatively low for a site near sources. One reason is that high terrain removes ozone equivalent to 3–5 DU. Another reason is frequent isolation from African pyrogenic ozone (section 6.3.3).

6.2. Interannual and Seasonal Variability in Time Versus Altitude Curtains

[34] Week-to-week variability over 1998–2000 at five SHADOZ sites (Ascension, Natal, Nairobi, Réunion, and Fiji) is depicted in time–altitude "curtain" plots (Figure 9). Sonde coverage at Irene, Watukosek, and San Cristóbal is more scattered than the stations shown.

[35] In early 1999 at Natal, Ascension, and Nairobi, in addition to clean marine air (~30 ppbv), layers of ozone >50 ppbv are found at 4–10 km in a number of soundings. An oceanographic cruise ("Aerosols99" ozone in Figure 10) in late January to early February 1999 showed that the high ozone over the south Atlantic may originate from several sources. Convective redistribution of clean marine air took place north of the Intertropical Convergence Zone (ITCZ) during the cruise (Figure 10) (profiles
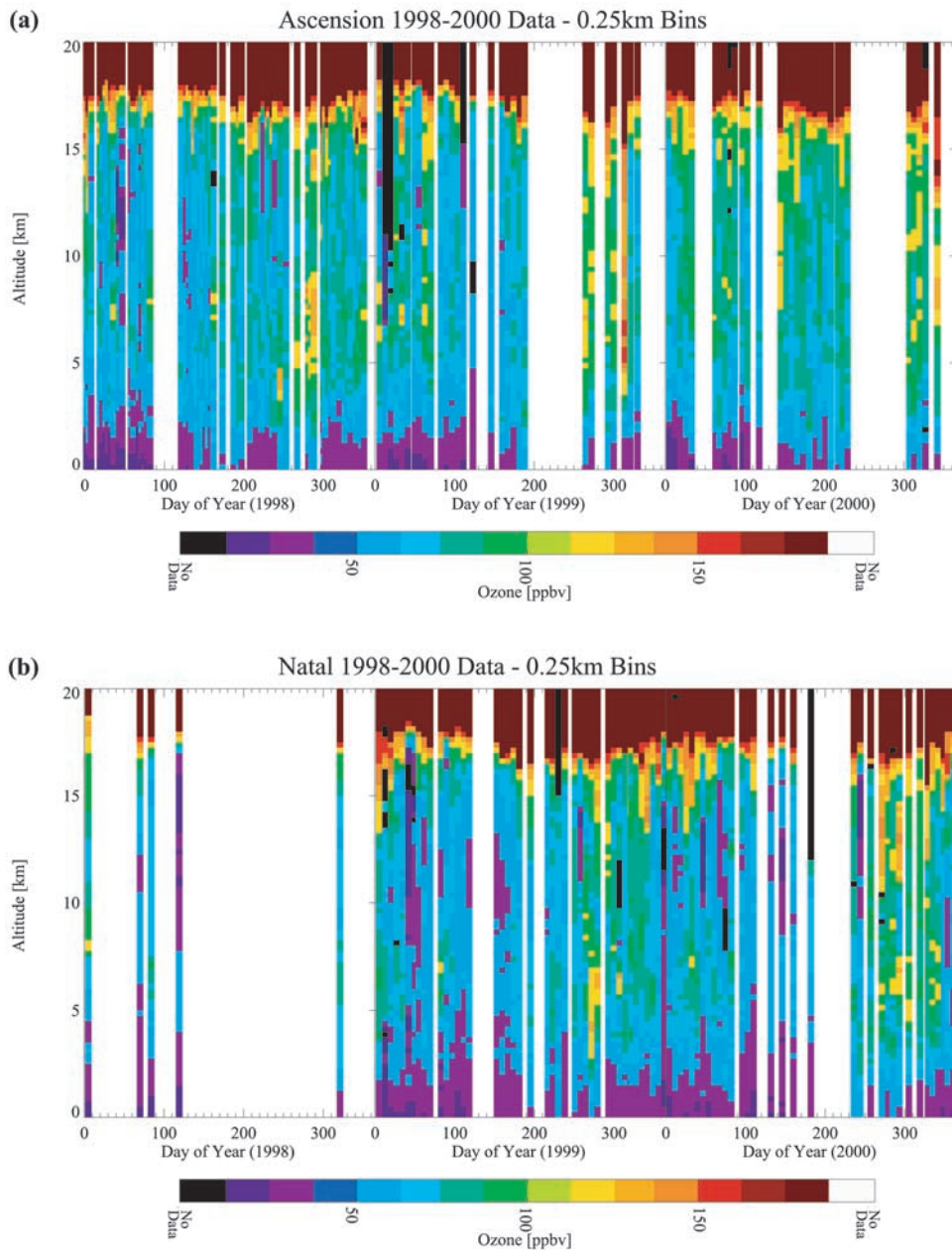
Figure 9.   Time versus altitude curtain of ozone mixing ratio (in ppbv) below 20 km based on 0.25 km averages. (a) Ascension, (b) Natal, (c) Nairobi, (d) Réunion, and (e) Fiji.

in the study of *Thompson et al.* [2000, Figure 3]). Pollution traceable to west African biomass burning was redistributed by convection at the ITCZ, detraining north and south of the convective zone to mix Northern and Southern Hemisphere air. The alternation of clean and polluted middle and upper tropospheric conditions over Ascension, Natal, and Nairobi (Figures 9a–9c) in January–March 1999 might also result from a variable ITCZ. W. Peters et al. (Tropospheric ozone over a tropical Atlantic station in the Northern Hemisphere: Paramaribo, Surinam (6N, 55W), submitted to *Tellus*, 2002, hereinafter referred to as Peters et al., submitted manuscript, 2002) report a similar phenomenon at Paramaribo, Surinam, in 2000, slightly north of the ITCZ (Figure 11a).

[36] It is likely that not all the midtroposphere high ozone observed at Natal, Ascension and Nairobi in early 1999 was due to pollution. During the Aerosols99 cruise, many high ozone layers sampled in the midtroposphere between 5°S and 15°S (cf. 5–12 km features at Ascension, Natal, and Nairobi) were accompanied by low water vapor [*Thompson et al.*, 2000, Figure 3] and subsidence of aged upper tropospheric air was inferred. When tropospheric ozone is higher in the nonburning Southern Hemisphere than in the actively burning Northern Hemisphere, a tropical Atlantic "ozone paradox" is said to occur (Figure 10).

[37] TRACE-A/SAFARI-92 aircraft sampling and sondes showed that Southern Hemisphere biomass burning in SON makes a contribution to lower and middle tropospheric ozone
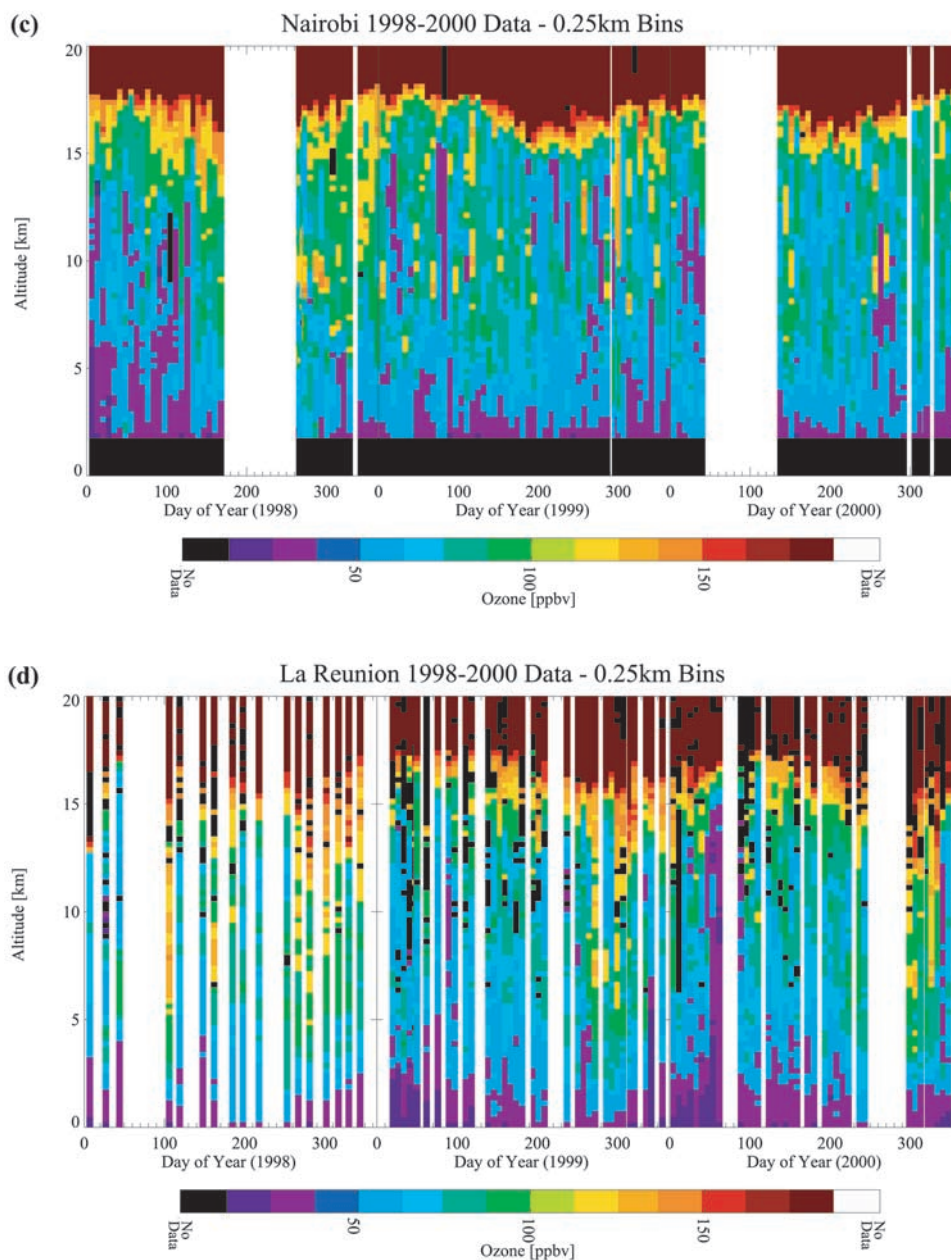
(c) Nairobi 1998-2000 Data - 0.25km Bins

(d) La Reunion 1998-2000 Data - 0.25km Bins

Figure 9. (continued)

at Ascension and Natal (green–yellow in Figures 9a and 9b in days 240–330) [*Browell et al.*, 1996; *Olson et al.*, 1996; *Thompson et al.*, 1996a]. Subsidence and recirculation of stratified air parcels over the south tropical Atlantic lead to greater column ozone over the ocean than over the continents (see the study of *Kim et al.* [1996] for a map). The upper troposphere at Natal and Ascension in SON is suggestive of these influences along with convective redistribution of ozone from biomass burning and ozone from lightning NO [*Pickering et al.*, 1996; *Thompson et al.*, 1997].

[38] Ozone over Nairobi and Réunion (Figures 9c and 9d) in March–May is more variable and, on average, greater in free tropospheric mixing ratio than over Natal or Ascension. The reason for this enhanced midtropospheric ozone (pronounced in 1999, less clear in 2000, when Nairobi has a

data gap) probably includes biomass burning from northern and central Africa. Although biomass burning over equatorial Africa peaks in December–February (north of the equator) and June–August (JJA, south of the equator), there is always enough fire activity over central Africa to affect Nairobi and Réunion. Réunion has a lower tropopause than the other SHADOZ stations (except for more southerly Irene) throughout the year, and upper tropospheric descent (yellow color, Figure 9d) is most pronounced between August and November.

[39] The pollution observed at Nairobi (Figure 9c) could originate from African burning and from India. Aircraft and shipboard soundings during INDOEX [*Lelieveld et al.*, 2001] and the Kaashidhoo ozonesondes archived in SHADOZ (Figure 11b) showed the Indian Ocean west of
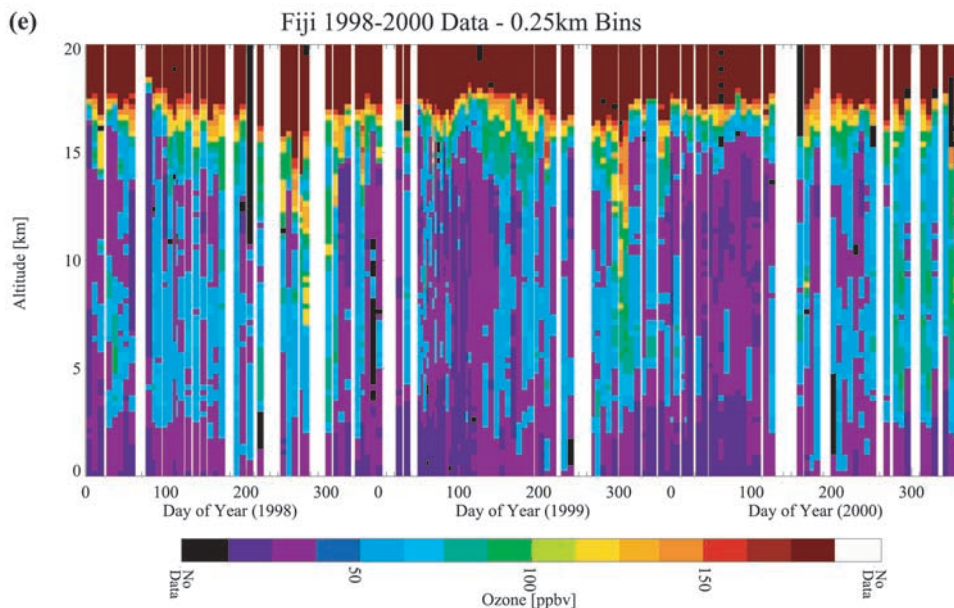
Figure 9.   (continued)

India to be very polluted in early 1999. The Kaashidhoo sondes captured ozone pollution layers hundreds to thousands of kilometers downwind from sources. High ozone levels are attributed to a variety of Indian sources [*Dickerson et al.*, 2002]. At other times, low ozone at higher altitudes suggests marine convection and less continental influence. Kaashidhoo pollution was prominent when several SHADOZ stations are least affected by biomass burning (e.g., Ascension and Natal). Clearly, a tropical ozone climatology from the fixed SHADOZ stations is not generally applicable to the northern tropics.

6.3. Processes Affecting Tropospheric Ozone

[40] Ozone time series (Figures 5, 6, and 9) point to multiple influences on ozone, e.g., convection, biomass burning, STE, lightning, and large-scale circulation (Walker and Hadley). Here we consider the influences of biomass burning, convection, and source locations for free tropospheric ozone seen in the SHADOZ soundings.

6.3.1. Biomass Burning

[41] Layers of elevated tropospheric ozone, particularly between the mixed layer and 300–400 hPa, are frequently traceable to biomass fires, especially during the Southern Hemisphere dry (burning) season. Figure 12 (dashed line) displays the seasonality of biomass burning using half-monthly averaged TOMS aerosol index (a proxy for biomass burning) for two regions covered by SHADOZ stations: the south tropical Atlantic and central Pacific. The satellite data are based on the Nimbus 7 record (1979–1992) [*Herman et al.*, 1997] which precedes the SHADOZ observing period. However, including the Earth-Probe record (1996 to present) in the statistics does not alter the seasonal cycle. Also shown is tropospheric ozone from the SHADOZ sondes taken within each region (stars for individual sondes).

[42] The sondes over Ascension (also Natal, not shown) between August and October fail to correlate simply with the biomass burning signal in Figure 12a, suggesting that dynamical factors play a role. Figures 9a and 9b show signs

of higher ozone mixing ratio in the upper troposphere, indicating greater subsidence (or stratospheric influence) over Ascension and Natal between August and October (section 4). Seasonal offsets are particularly pronounced over the Atlantic where they were noted during TRACE-A [*Thompson et al.* 1996a, 1996b; *Olson et al.*, 1996] and the Aerosols99 cruise [*Thompson et al.*, 2000, 2001].

6.3.2. Convective Influences

[43] To examine convective influences in SHADOZ ozone, precipitation and lightning data from the Tropical
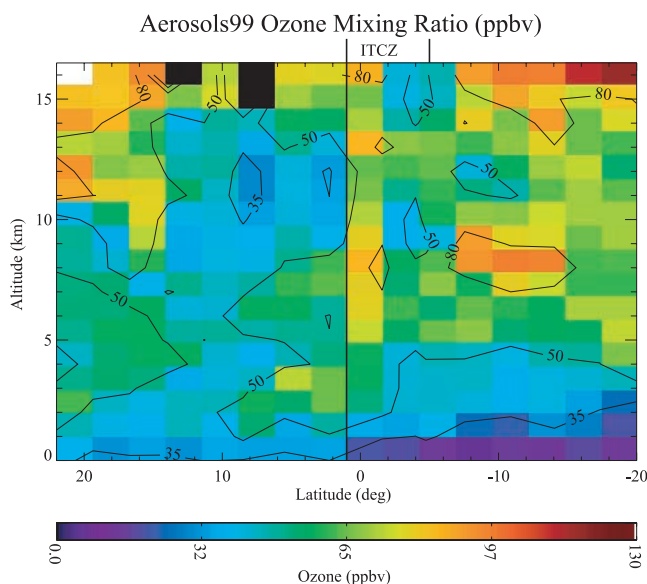

Figure 10.   Ozone mixing ratio in 1 km averages (35, 50, and 80 ppbv contours included) from Aerosols99 cruise launches between 20°N and 20°S (23 January to 4 February 1999). Ozone soundings were taken by shipboard launches between Norfolk (US) to South Africa. ITCZ range indicated above.
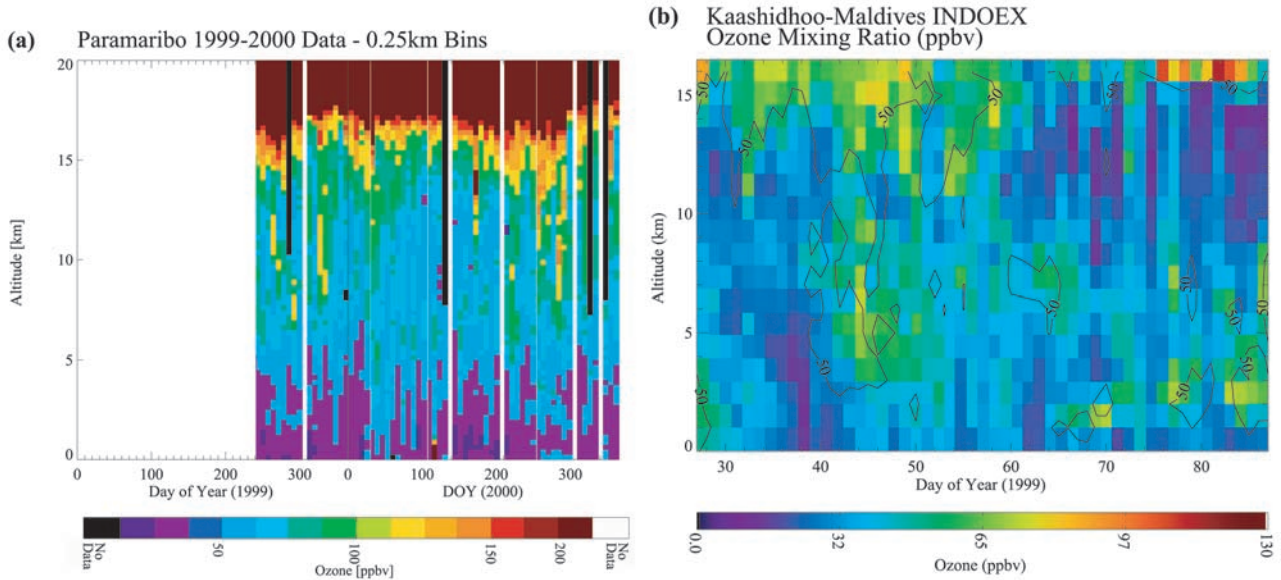
Figure 11. Time versus altitude curtain of ozone mixing ratio (in ppbv) below 20 km based on 0.25 km averages for (a) Paramaribo, station that started during 1999. (b) INDOEX campaign launches at Kaashidhoo (on Male, Maldives, 5°N, 75°E) for which 50 ppbv contour shown.

Rainfall Measuring Mission (TRMM) satellite (1997) [*Adler et al.*, 2000] were assembled. The correlation was not strong. The reason could be the averaging required to obtain good TRMM statistics. Thus, we summarize convective influences using the appearance of low ozone (<20 ppbv, in time versus altitude curtains) as follows:

1. *Ascension* (Figure 9a) has the least convective influence of SHADOZ sites.

2. *Natal*. Low ozone (purple, Figure 9b) and upper troposphere or lower stratospheric influence occur often between 5 and 17 km. The DJF convective influence can last until May. For example, in December 1998 to May

1999, even though north central African burning may add high-ozone layers between 3 and 12 km, convection influences ozone up to 15 km.

3. *Nairobi* (Figure 9c) has the greatest convective influence in early 1998, similar to Réunion, although the latter has fewer sondes for comparison. After 1998, there is little effect of convection on ozone until early 2000.

4. *Réunion*. Although the general characteristics seen at Nairobi hold at Réunion (Figure 9d), this station is more diverse with middle to late 1998 heavy in stratospheric influence and some convective influence in 2000.

5. *Fiji* (Figure 9e) shows heavy convective influence, routinely reaching 15 km in the first 100 days of each year.
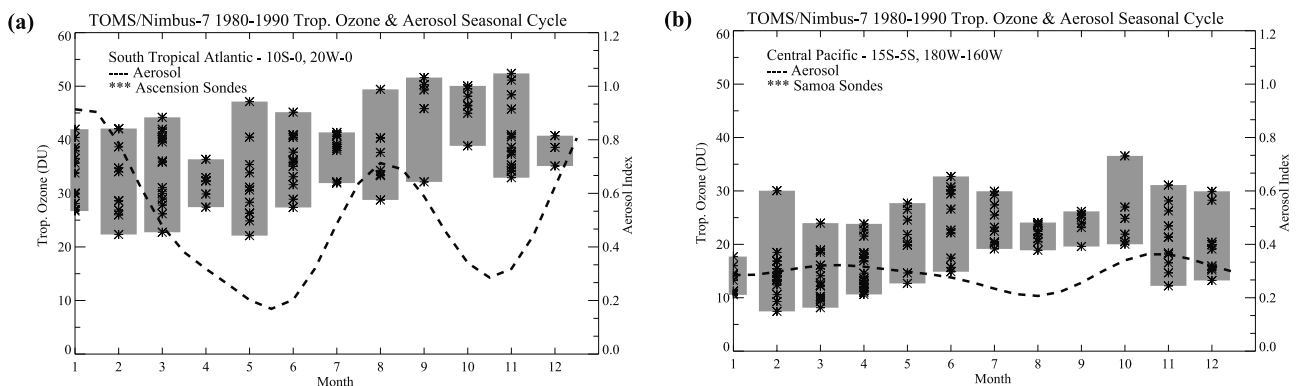

Figure 12. Statistically determined annual cycle of TOMS absorbing aerosol (dashed) using 11 years (1980–1990) of Nimbus 7/TOMS satellite measurements (see the study of *Thompson et al.* [2001] for description of calculation). Within each region, integrated tropospheric ozone from sondes at a representative station are shown (stars, gray shading indicating range of maximum and minimum values). Regional averages: (a) south tropical Atlantic, mean region = 0°–10°S, 0°–20°W, Ascension station and (b) central Pacific (5°–15°S, 160°–180°W) with Samoa sondes. The eastern Pacific (San Cristóbal) and Indonesian maritime continent (Watukosek) are similar to the ozone and aerosol patterns over the central Pacific.
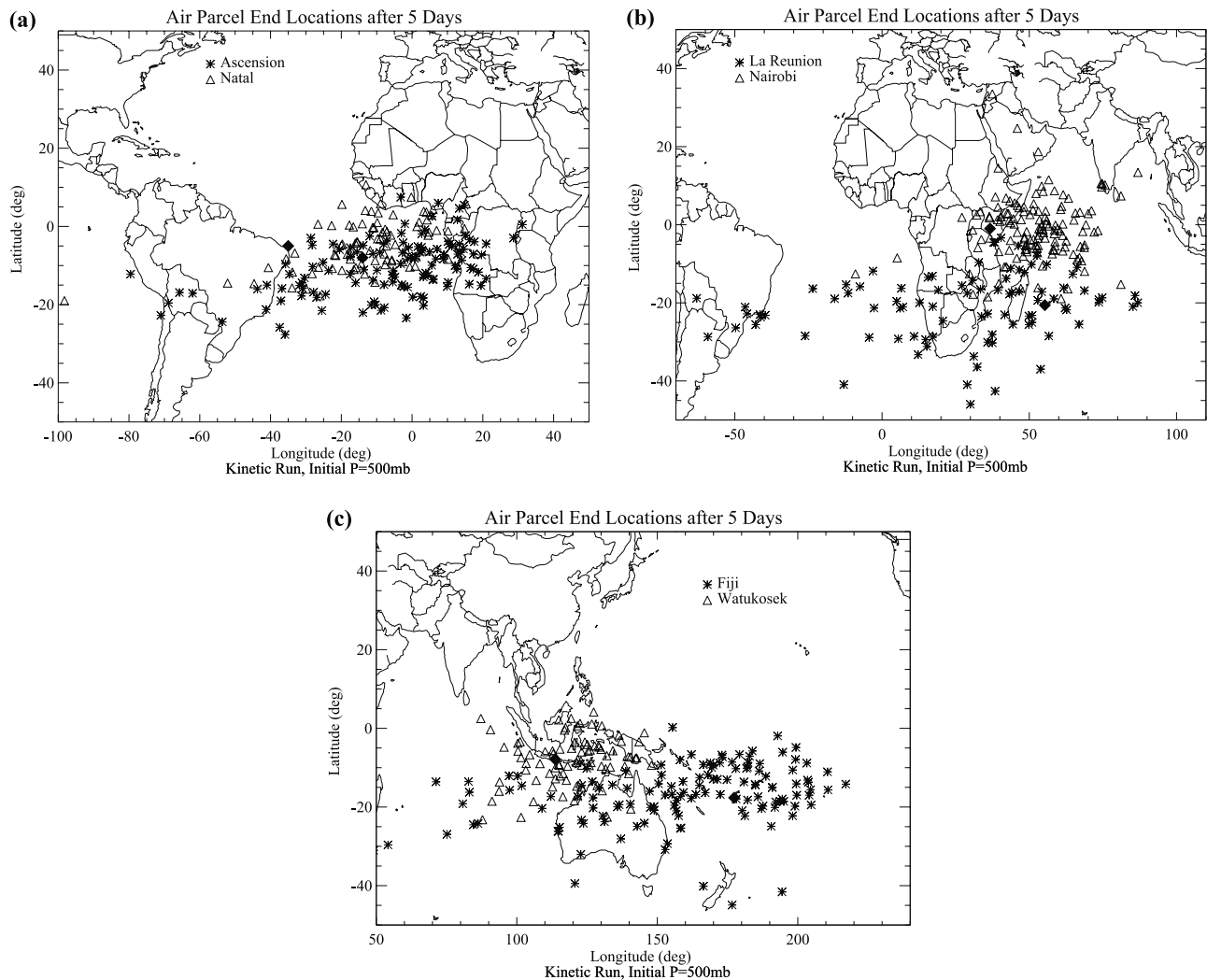
(a)
Air Parcel End Locations after 5 Days

(b)
Air Parcel End Locations after 5 Days

(c)
Air Parcel End Locations after 5 Days

Figure 13. Origins of air parcel back-trajectories initialized at 500 hPa from eight station locations for all 1998–2000 launches and run for 5 days. NASA Goddard kinematic trajectory model used with NCEP 2.5 × 2.5 gridded wind fields. Station location (filled diamond) is indicated. (a) Ascension and Natal, (b) Réunion and Nairobi, and (c) Fiji and Watukosek.

6. *Paramaribo* (Figure 11a) shows convective influence, up to 13–15 km related to the ITCZ passing over, during December and January and April–July, corresponding to the short and long, wet season (W. Peters et al., submitted manuscript, 2002).

6.3.3. Midtroposphere Trajectory Origins

[44] The NASA/Goddard kinematic trajectory model [*Schoeberl and Newman*, 1995] is used to examine source regions for midtropospheric ozone. Figure 13 shows the origin points of 5-day back-trajectories that were initialized for each launch date at 500 hPa. End pressures corresponded to 325–450 hPa and the latitude–longitude of the origin after 5 days is marked. How does the trajectory climatology (TC) for each point correspond to the picture deduced from the altitude versus time curtains? Ascension and Natal (Figure 13a) air parcel origins somewhat resemble one another; the two stations are within 2° latitude of one another. Ascension origins are displaced farther east and south, over Africa and the eastern Atlantic, where tropo-spheric ozone is on average at its highest tropical value [*Thompson and Hudson*, 1999]. The TC for Natal has origins farther north in the Atlantic, consistent with Natal showing more signs of the ITCZ, i.e., midtropospheric ozone <40 ppbv.

[45] The Nairobi cluster of origin points (Figure 13b) is confined to 40°–80°E, a region that may be influenced by pollution from nearby African countries or India [*Lelieveld et al.*, 2001]. Nairobi origins are approximately half polluted and half clean, as the individual profiles show (see section 5). Réunion (Figure 13b) shows diffuse trajectory origins and end points farther away, as far as South America. However, the greatest clustering of Réunion origins is over Africa, the eastern Indian Ocean and Madagascar. These locations are subject to stratospheric and biomass burning influences [*Taupin et al.*, 1999; *Randriambelo et al.*, 2000]. Central Indian Ocean origins for Réunion occur frequently in December–March; these correspond to the lowest UT ozone in 1999 and 2000.

[46] To put Fiji TC (Figure 13c) into context, it helps to look at the TC for Watukosek. Watukosek origins do not coincide with those from Réunion or Nairobi (sites to the east) nor with San Cristóbal to the east. Fiji has a few air parcel origins within range of those arriving at Réunion and some overlap with Watukosek in the eastern Indian Ocean and over Australia. Fiji origins (and Samoa origins, not shown) are heavily marine, i.e., over the western Pacific in the vicinity of the SPCZ [*Pickering et al.*, 2001].

7. Summary

[47] Over 1100 soundings from the Southern Hemisphere tropics and subtropics give an overview of tropical ozone during the 1998–2000 period. Time series of individual ozone profiles and column-integrated ozone (total, stratospheric, and tropospheric) amounts show:

1. Normal Southern Hemisphere patterns, higher ozone throughout the column during the second half of the year compared to the first half. Stratospheric column ozone is typically 10–20 DU higher in September–November than in March–May. Stratospheric ozone profiles show that the first 3 years of SHADOZ data cover an entire QBO cycle (Logan et al., submitted manuscript, 2002).

2. The zonal wave-one pattern seen in satellite ozone (referring to 10–15 DU more ozone over the Atlantic–African–western Indian Ocean region than over the eastern Indian Ocean–western Pacific) can be seen in the SHADOZ tropospheric ozone record throughout the year. The magnitude of the wave is greatest in SON, when downwelling from the upper troposphere concentrates ozone over the Atlantic, where it is further enhanced by ozone transported and recirculated from African burning regions and from lightning-produced NO.

3. Tropospheric ozone varies up to a factor of 3 in column amount over the course of the year at all but two SHADOZ sites. Very clean and polluted conditions alternate; the most persistent pollution is found at Réunion, Natal, Ascension, and Fiji, sites where biomass burning impacts from Africa occur several months each year. Seasonal and monthly mean tropospheric ozone amounts are of marginal statistical value because distributions are often not Gaussian. There is a characteristic minimum at each station.

4. A comparison between SHADOZ data and ozone profiles used in BUV satellite retrievals shows the limitations of the latter with respect to ozone variability. Errors in the tropospheric profile at the cleanest and most polluted stations may be substantial. Tropical satellite algorithms must incorporate longitudinal and seasonal variations in the climatology.

5. Dynamic signals apparent in individual soundings include the varying ITCZ, regional convective influence, and the ENSO–La Niña transition in 1998–1999. A comparison of tropospheric ozone amounts and biomass burning seasonality does not match at most SHADOZ sites. The inference is that dynamics controls much of the ozone distribution, similar to evidence from the "ozone paradox" [*Thompson et al.*, 2000].

[48] The SHADOZ data show complex interactions between tropospheric ozone and dynamics, with the latter possibly dominating over the influences of fires and lightning. More definitive quantification of ozone sources requires model interpretation. The limited SHADOZ data from the northern tropics are quite distinct from the Southern Hemisphere stations and argue for expansion of observations north of the equator.

References

Adler, R. F., G. J. Huffman, D. T. Bolvin, S. Curtis, and E. J. Nelkin, Tropical rainfall distributions determined using TRMM combined with other satellite and raingauge information, *J. Appl. Meteorol.*, *39*, 2007–2023, 2000.

Baldwin, M. P., et al., The quasi-biennial oscillation, *Rev. Geophys.*, *39*, 179–229, 2001.

Baldy, S., G. Ancellet, M. Bessafi, A. Badr, and D. Lan Sun Luk, Field observations of the vertical distribution of tropospheric ozone at the island of Reunion (southern tropics), *J. Geophys. Res.*, *101*, 23,835–23,849, 1996.

Bojkov, R. D., and V. E. Fioletov, Total ozone variations in the tropical belt: An application for quality of ground based measurements, *Meteorol. Atmos. Phys.*, *58*, 223–240, 1996.

Bowman, K., Global patterns of the quasi-biennial oscillation in total ozone, *J. Atmos. Sci.*, *46*, 3328–3342, 1989.

Browell, E. V., et al., Ozone and aerosol distributions and air mass characteristics over the South Atlantic basin during the burning season, *J. Geophys. Res.*, *101*, 24,043–24,068, 1996.

Chane-Ming, F., F. Molinaro, J. Leveau, P. Keckhut, A. Hauchecorne, and S. Godin, Vertical short-scale structures in the upper tropospheric-lower stratospheric temperature and ozone at La Réunion Island (20.8°S, 55.3°E), *J. Geophys. Res.*, *105*, 26,857–26,866, 2000.

Dickerson, R. R., M. O. Andreae, T. Campos, O. L. Mayol-Bracero, C. Neuseuss, and D. G. Streets, Analysis of black carbon and carbon monoxide observed over the Indian Ocean: Implications for emissions and photochemistry, *J. Geophys. Res.*, *107*, 8017, doi:10.1029/2001JD000501, 2002.

Folkins, I., M. Loewenstein, J. Podolske, S. J. Oltmans, and M. Proffitt, A barrier to vertical mixing at 14 km in the tropics: Evidence from ozonesondes and aircraft measurements, *J. Geophys. Res.*, *104*, 22,095–22,102, 1999.

Folkins, I., S. J. Oltmans, and A. M. Thompson, Tropical convective outflow and near-surface equivalent potential temperatures, *Geophys. Res. Lett.*, *27*, 2549–2552, 2000.

Folkins, I., C. Braun, A. M. Thompson, and J. C. Witte, Tropical ozone as in indicator of deep convective outflow, *J. Geophys. Res.*, *107*, 4184, doi:10.1029/2001JD001178, 2002.

Fujiwara, M., K. Kita, S. Kawakami, T. Ogawa, N. Komala, S. Saraspriya, and A. Suripto, Tropospheric ozone enhancements during the Indonesian forest fire events in 1994 and in 1997 as revealed by ground-based observations, *Geophys. Res. Lett.*, *26*, 2417–2420, 1999.

Fujiwara, M., K. Kita, T. Ogawa, S. Kawakami, T. Sano, N. Komala, S. Saraspriya, and A. Suripto, Seasonal variation of tropospheric ozone in Indonesia revealed by 5-year ground-based observations, *J. Geophys. Res.*, *105*, 1879–1888, 2000.

Hansen, J. E., et al., Climate forcings in GISS SI2000 simulations, *J. Geophys. Res.*, *107*, 4347, doi:10.1029/2001JD001143, 2002.

Hasebe, F., Quasi-biennial oscillations of ozone and diabatic circulation in the equatorial stratosphere, *J. Atmos. Sci.*, *51*, 729–745, 1994.

Herman, J. R., P. K. Bhartia, O. Torres, C. Hsu, C. Seftor, and E. Celarier, Global distributions of UV-absorbing aerosols from Nimbus 7/TOMS data, *J. Geophys. Res.*, *102*, 16,911–16,922, 1997.

Hollandsworth, S. M., R. D. McPeters, L. E. Flynn, W. Planet, A. J. Miller, and S. Chandra, Ozone trends deduced from combined Nimbus 7 SBUV and NOAA 11 SBUV/2 data, *Geophys. Res. Lett.*, *22*, 905–908, 1995.

Hudson, R. D., J. H. Kim, and A. M. Thompson, On the derivation of tropospheric column ozone from radiances measured by the total ozone mapping spectrometer, *J. Geophys. Res.*, *100*, 11,138–11,145, 1995.

Johnson, B. J., S. J. Oltmans, H. Vömel, T. Deshler, C. Kroger, and H. G. J. Smit, Electrochemical concentration cell (ECC) ozonesonde pump efficiency measurements and tests on the sensitivity to ozone of buffered and unbuffered ECC sensor cathode solutions, *J. Geophys. Res.*, *107*, 4393, doi:10.1029/2001JD000557, 2002.

Kalnay, E., et al., The NCEP/NCAR 40-year re-analysis project, *Bull. Am. Meteorol. Soc.*, *77*, 437–471, 1996.

Kim, J. H., R. D. Hudson, and A. M. Thompson, A new method of deriving time-averaged tropospheric column ozone over the tropics using total ozone mapping spectrometer (TOMS) radiances: Intercomparison and analysis using TRACE A data, *J. Geophys. Res.*, *101*, 24,317–24,330, 1996.

Kirchhoff, V. W. J. H., I. M. O. Dasilva, and E. V. Browell, Ozone measurements in Amazonia: Dry season versus wet season, *J. Geophys. Res.*, *95*, 16,913–16,926, 1990.

Kirchhoff, V. W. J. H., R. A. Barnes, and A. L. Torres, Ozone climatology at Natal, Brazil, from in situ ozonesonde data, *J. Geophys. Res.*, *96*, 10,899–10,909, 1991.

Kirchhoff, V. W. J. H., J. R. Alves, F. R. da Silva, and J. Fishman, Observations of ozone concentrations in the Brazilian cerrado during the TRACE-A field expedition, *J. Geophys. Res.*, *101*, 24,029–24,042, 1996.

Klenk, F. K., P. K. Bhartia, A. J. Fleig, V. G. Kaveeshwar, R. D. McPeters, and P. M. Smith, Total ozone determination from the Backscattered Ultraviolet (BUV) experiment, *J. Appl. Meteorol.*, *21*, 1672–1684, 1982.

Kobayashi, J., and Y. Toyama, On various methods of measuring the vertical distribution of atmospheric ozone (III) carbon–iodine type chemical ozonesonde, *Pap. Meteorol. Geophys.*, *17*, 113–126, 1966.

Komala, N., S. Saraspriya, K. Kita, and T. Ogawa, Tropospheric ozone behavior observed in Indonesia, *Atmos. Environ.*, *30*, 1851–1856, 1996.

Komhyr, W. D., Operations Handbook: Ozone measurements to 40 km altitude with model 4A-ECC-ozone sondes, *NOAA Tech. Memo. ERL-ARL-149*, 1986.

Komhyr, W. D., R. A. Barnes, G. B. Brothers, J. A. Lathrop, and D. P. Opperman, Electrochemical concentration cell ozonesonde performance during STOIC 1989, *J. Geophys. Res.*, *100*, 9231–9244, 1995.

Kondo, Y., M. Ko, M. Koike, S. Kawakami, and T. Ogawa, Preface to Special Section on Biomass Burning and Lightning Experiment (BIBLE), *J. Geophys. Res.*, *107*, 8397, doi:10.1029/2002JD002401, 2002 [printed *108*(D3), 2003].

Krishnamurti, T. N., M. C. Sinha, M. Kanamitsu, D. Oosterhof, H. Fuelberg, R. Chatfield, D. J. Jacob, and J. Logan, Passive tracer transports relevant to the TRACE-A experiment, *J. Geophys. Res.*, *101*, 23,889–23,908, 1996.

Lelieveld, J., et al., The Indian Ocean Experiment: Widespread air pollution from South and Southeast Asia, *Science*, *291*, 1031–1036, 2001.

Logan, J. A., An analysis of ozonesonde data for the troposphere: Recommendations for testing three-dimensional models and development of a gridded climatology for tropospheric ozone, *J. Geophys. Res.*, *104*, 16,115–16,149, 1999a.

Logan, J. A., An analysis of ozonesonde data for the lower stratosphere: Recommendations for testing models, *J. Geophys. Res.*, *104*, 16,151–16,170, 1999b.

Logan, J. A., and V. W. J. H. Kirchhoff, Seasonal variations of tropospheric ozone at Natal, Brazil, *J. Geophys. Res.*, *91*, 7875–7881, 1986.

Martin, R. V., D. J. Jacob, J. A. Logan, J. M. Ziemke, and R. Washington, Detection of a lightning influence on tropical tropospheric ozone, *Geophys. Res. Lett.*, *27*, 1639–1642, 2000.

Martin, R. V., et al., Interpretation of TOMS observations of tropical tropospheric ozone with a global model in situ observations, *J. Geophys. Res.*, *107*(D18), 4351, doi:10.1029/2001JD001480, 2002.

McPeters, R. D., G. J. Labow, and B. J. Johnson, A satellite-derived ozone climatology for balloonsonde estimation of total column ozone, *J. Geophys. Res.*, *102*, 8875–8885, 1997.

Moxim, W. J., and H. Levy II, A model analysis of the tropical South Atlantic Ocean tropospheric ozone maximum: The interaction of transport and chemistry, *J. Geophys. Res.*, *27*, 17,393–17,416, 2000.

Newchurch, M. J., D. Sun, and J. H. Kim, Zonal wave-1 structure in TOMS tropical stratospheric ozone, *Geophys. Res. Lett.*, *28*, 3151–3154, 2001.

Newell, R. E., V. Thouret, J. Y. N. Cho, P. Stoller, A. Marenco, and H. G. Smit, Ubiquity of quasi-horizontal layers in the troposphere, *Nature*, *398*, 316–319, 1999.

Olson, J. R., J. Fishman, V. W. J. H. Kirchhoff, D. Nganga, and B. Cros, Analysis of the distribution of ozone over the southern Atlantic region, *J. Geophys. Res.*, *101*, 24,083–24,094, 1996.

Oltmans, S. J., et al., Ozone in the Pacific tropical troposphere from ozonesonde observations, *J. Geophys. Res.*, *106*, 32,503–32,526, 2001.

Pickering, K. E., et al., Convective transport of biomass burning emissions over Brazil during TRACE A, *J. Geophys. Res.*, *101*, 23,993–24,012, 1996.

Pickering, K. E., et al., Trace gas transport and scavenging in PEM-Tropics-B South Pacific Convergence Zone convection, *J. Geophys. Res.*, *106*, 32,591–32,608, 2001.

Randel, W. J., and F. Wu, Isolation of the ozone QBO in SAGE II data by singular-value decomposition, *J. Atmos. Sci.*, *53*, 2546–2559, 1996.

Randriambelo, T., J.-L. Baray, and S. Baldy, Effect of biomass burning, convective venting, and transport on tropospheric ozone over the Indian Ocean: Reunion Island field observations, *J. Geophys. Res.*, *105*, 11,813–11,832, 2000.

Reed, R. J., A tentative model of the 26-month oscillation in tropical latitudes, *Q. J. R. Meteorol. Soc.*, *90*, 441–446, 1964.

Saji, N. H., B. N. Goswami, P. N. Vinayachandran, and T. Yamagata, A dipole mode in the tropical Indian Ocean, *Nature*, *401*, 360–363, 1999.

Schoeberl, M. R., and P. A. Newman, A multiple-level trajectory analysis of vortex filaments, *J. Geophys. Res.*, *100*, 25,801–25,815, 1995.

Shiotani, M., Annual, quasi-biennial and El Nino–Southern Oscillation (ENSO) time-scale variations in equatorial total ozone, *J. Geophys. Res.*, *97*, 7625–7634, 1992.

Smit, H., D. Kley, S. McKeen, A. Volz, and S. Gilge, The latitudinal and vertical distribution of tropospheric ozone over the Atlantic Ocean in the southern and northern hemispheres, in *Ozone in the Atmosphere: Proceedings of the Quadrennial Ozone Symposium 1988 and Tropospheric Ozone Workshop*, edited by R. D. Bojkov and P. Fabian, pp. 419–422, A. Deepak, Hampton, Va., 1989.

Swap, R. J., et al., The Southern African Regional Science Initiative (SAFARI-2000): Dry-season field campaign, An overview, *S. Afr. J. Sci.*, *98*, 125–130, 2002.

Taupin, F. G., M. Bessafi, S. Baldy, and P. J. Bremaud, Tropospheric ozone above the southwestern Indian Ocean is strongly linked to dynamical conditions prevailing in the tropics, *J. Geophys. Res.*, *104*, 8057–8066, 1999.

Thompson, A. M., and R. D. Hudson, Tropical tropospheric ozone (TTO) maps from Nimbus 7 and Earth Probe TOMS by the modified-residual method: Evaluation with sondes, ENSO signals, and trends from Atlantic regional time series, *J. Geophys. Res.*, *104*, 26,961–26,975, 1999.

Thompson, A. M., K. E. Pickering, D. P. McNamara, M. R. Schoeberl, R. D. Hudson, J. H. Kim, E. V. Browell, V. W. J. H. Kirchhoff, and D. Nganga, Where did tropospheric ozone over southern Africa and the tropical Atlantic come from in October 1992? Insights from TOMS, GTE TRACE A and SAFARI 1992, *J. Geophys. Res.*, *101*, 24,251–24,278, 1996a.

Thompson, A. M., et al., Ozone over southern Africa during SAFARI-92/TRACE A, *J. Geophys. Res.*, *101*, 23,793–23,807, 1996b.

Thompson, A. M., W.-K. Tao, K. E. Pickering, J. R. Scala, and J. Simpson, Tropical deep convection and ozone formation, *Bull. Am. Meteorol. Soc.*, *78*, 1043–1054, 1997.

Thompson, A. M., B. G. Doddridge, J. C. Witte, R. D. Hudson, W. T. Luke, J. E. Johnson, B. J. Johnson, S. J. Oltmans, and R. Weller, A tropical Atlantic ozone paradox: Shipboard and satellite views of a tropospheric ozone maximum and wave-one in January–February 1999, *Geophys. Res. Lett.*, *27*, 3317–3320, 2000.

Thompson, A. M., J. C. Witte, R. D. Hudson, H. Guo, J. R. Herman, and M. Fujiwara, Tropical tropospheric ozone and biomass burning, *Science*, *291*, 2128–2132, 2001.

Thompson, A. M., et al., Southern Hemisphere Additional Ozonesondes (SHADOZ) 1998–2000 tropical ozone climatology, 1, Comparison with TOMS and ground-based measurements, *J. Geophys. Res.*, doi:10.1029/2001JD000967, in press, 2002a.

Thompson, A. M., J. C. Witte, M. T. Freiman, N. A. Phahlane, and G. J. R. Coetzee, Lusaka, Zambia, during SAFARI-2000: Convergence of local and imported ozone pollution, *Geophys. Res. Lett.*, *29*, 1976, doi:10.1029/2002GL015,399, 2002b.

Wang, W.-C., J. P. Pinto, and Y. L. Yung, Climatic effects due to halogenated compounds in the Earth's atmosphere, *J. Atmos. Sci.*, *37*, 333–338, 1980.

Wang, W.-C., Y.-C. Zhuang, and R. D. Bojkov, Climate implications of observed changes in ozone vertical distributions at middle and high latitudes of the Northern Hemisphere, *Geophys. Res. Lett.*, *20*, 1567–1570, 1993.

Webster, P. W., A. M. Moore, J. P. Loschnigg, and R. R. Leben, Coupled ocean-atmosphere dynamics in the Indian Ocean during 1997–98, *Nature*, *401*, 356–360, 1999.

Weller, R., R. Lilischkis, O. Schrems, R. Neuber, and S. Wessel, Vertical ozone distribution in the marine atmosphere over the central Atlantic Ocean (56°S–50°N), *J. Geophys. Res.*, *101*, 1387–1399, 1996.

World Meteorological Organization, SPARC/IOC/GAW Assessment of trends in the vertical distribution of ozone, edited by N. Harris et al., *SPARC Rep. 1, Rep. 43*, WMO Global Ozone Res. and Monit. Proj., Geneva, 1998.

Zawodny, J., and M. P. McCormick, Stratospheric aerosol and gas experiment II measurements of the quasi-biennial oscillations in ozone and nitrogen oxide, *J. Geophys. Res.*, *96*, 9371–9377, 1991.

———————————

G. J. R. Coetzee, South African Weather Bureau, PB X097, Pretoria 0001, South Africa.

J. P. F. Fortuin and H. M. Kelder, Royal Netherlands Meteorological Institute (KNMI), De Bilt, Netherlands.

M. Fujiwara, Radio Science Center for Space and Atmosphere, Kyoto University, Kyoto, Japan.

B. Hoegger, Swiss Aerological Observatory, Méteo-Suissem, Payerene, Switzerland.

S. Kawakami and T. Ogawa, NASDA Earth Observations Research Center, Tokyo, Japan.

V. W. J. H. Kirchhoff, INPE Laboratorio de Ozonio, São José dos Campos, Brazil.

J. A. Logan, Harvard University, Cambridge, MA 02138, USA.

S. J. Oltmans, NOAA Climate Monitoring and Diagnostics Laboratory, Boulder, CO 80305, USA.

F. Posny, Université de la Réunion, St-Denis, Réunion France.

F. J. Schmidlin, NASA Wallops Flight Facility, Mail Code 972, Wallop Is., VA 23337, USA.

A. M. Thompson, Atmospheric Chemistry and Dynamics Branch, NASA Goddard Space Flight Center, Building 33, Room E417, Mail Code 916, Greenbelt, MD 20771, USA. (anne.m.thompson@nasa.gov)

J. C. Witte, Science Systems and Applications, Inc. (SSAI), NASA Goddard Space Flight Center, Greenbelt, MD 20771, USA.